

ALMA MATER STUDIORUM - UNIVERSITÀ DI BOLOGNA

SCUOLA DI INGEGNERIA E ARCHITETTURA

DIPARTIMENTO di INGEGNERIA DELL'ENERGIA ELETTRICA E
DELL'INFORMAZIONE "Guglielmo Marconi" DEI

**CORSO DI LAUREA MAGISTRALE IN INGEGNERIA
DELL'ENERGIA ELETTRICA**

TESI DI LAUREA
in Compatibilità Elettromagnetica e Laboratorio T

**MEASUREMENT AND SIMULATION OF
CONDUCTED DISTURBANCES ON DC POWER
GRIDS OF A HVDC SYSTEM WITH AN ACTIVE
DC/DC CONVERTER**

CANDIDATO

Luca Ensini

RELATORE

Prof. Leonardo Sandrolini

CORRELATORE

Prof. Dave W.P. Thomas
Prof. Mark Sumner

Anno Accademico
2016/2017

Sessione
III

INDEX

INTRODUCTION	2
1. DC SYSTEMS	5
1.1 DC-Microgrid	5
1.2 HVDC (High Voltage Direct Current)	8
2. CONVERTERS	12
2.1 DC/DC Converters - Buck Converter	13
2.2 HVDC Converters	18
3. MEASURING AND ELABORATION METHODS FOR CONDUCTED EMISSIONS WITHIN THE RANGE 2-150kHz	22
3.1 Line Impedance Stabilization Network (LISN)	23
3.2 Fourier Transform (FT)	26
3.3 Short Time Fourier Transform (STFT)	32
3.4 Amplitude Probability Distribution (APD)	34
4. DC POWER QUALITY PARAMETERS AND STANDARD EMISSION LIMITS WITHIN THE RANGE 2-150kHz	37
4.1 DC Power Quality Parameters	38
4.2 Standard Emission Limits within the Range 2-150kHz	41
5. CONVERTER CONDUCTED EMISSIONS MEASUREMENT	42
5.1 Measurement Setup and its Description	42
5.2 MATLAB Scripts	48
5.3 Measurement Results	51
6. CONDUCTED EMISSIONS MEASUREMENT SIMULATION	60
6.1 Simulation Circuit	60
6.2 MATLAB Scripts	64
6.3 Simulation Results	67
7. CONCLUSIONS	84
8. BIBLIOGRAPHY	86

INTRODUCTION

In the last years, with the increasing of the distributed generation, DC microgrids have become more and more common in the electrical network. Distributed generation means renewable energy, of small and large dimension, connected then to the main electrical network. With renewable energy we consider wind-energy, geothermal-energy, biomass-energy, but, in most cases, distributed generation means solar-energy; this because now, finding buildings with solar cells in their roofs or bigger solar rig in open fields is very easy.

Lately, more solar production rigs have been connected together, also with their loads, making, in this way, microgrids; as known, photovoltaic cells produce direct voltage and current, so we can talk about DC-microgrids. To connect these rigs to the network, it is necessary to use converters from Direct Current (DC) to Alternative Current (AC). Furthermore, the control of this kind of generation is made with DC-DC converter, due to the fact that the output of a solar cell changes with different weather, and to manage the power flows and the voltage levels within the microgrids.

The use of direct current is becoming more likely to find also in the transmission of electricity at high voltage, named High Voltage Direct Current (HVDC), mainly where it is necessary to connect large regions or countries (for example from Italy and Greek, or Italy and Switzerland). HVDC become preferable than HVAC (High Voltage Alternative Current) when the transmission line become long because the higher cost of DC terminals are compensated by the lower DC line cost and lower DC losses. DC terminals consist in AC-DC converters which are necessary to connect these lines to the AC network.

All these converters work at high frequencies producing noise, harmonics, disturbances that might damage or, at least, get worse the function of other connected equipment, which can be generators of disturbances too, being often linked with the microgrids with converters.

Often, the switching frequencies of these converters are in the frequency range between 2-150kHz where recognized standard disturbance limits and standard disturbance measurement methods do not exist yet, although a few have been proposed. It might be interesting trying to find new methods of measurement to compare with the proposed standard. One method could be using the LISN (Line

Impedance Stabilization Network), connected to a receiver, which is normally used for emission measurements in the range 150kHz-30MHz. The main purpose of this instrument is to have a standard for every measurements, stabilizing the impedance seen by the receiver, filtering the noise from the network, letting pass the 50-60Hz component (DC in this case) to supply the equipment under test (EUT) and filtering and measuring the noise from the EUT.

After the measurement in time domain, frequency domain and time-frequency domain studies might be interesting. In fact, with time domain studies it is possible to calculate some Power Quality (PQ) parameters of the signal and it is possible to see the time variation of the signal, but if we want to know the harmonic components of it we have to elaborate the signal. To achieve this purpose, Fourier Transform is used. In this work, a variation of the Fourier transform is used, the Fast Fourier Transform (FFT), which uses an algorithm to make it faster. Often the signals and the disturbance signals, also in DC, are not steady state, because the loads and system conditions change, and that is the reason why time-frequency domain studies become important. To do this, Short Time Fourier Transform (STFT) is used. The main difference between STFT and FFT is that STFT does the Fourier transform not of the entire measured signal, but it split the signal in more windows in time domain and then it applies the Fourier transform to each window. In this way is possible to see how the signal and the related harmonic components vary during the acquisition time. To do the STFT is possible to split the time domain signal in more windows of equal time and then doing the FFT of each time segment, or, if MATLAB is used to elaborate the signal, there is the function "Spectrogram" that does the STFT directly. Normally a rectangular window is used, but, sometimes problems can occur, so different kind of windowing might be used taking in account that the windowing might be a generator of calculating problems, too. Power quality parameters are of different types: there are time-domain parameters as the average DC component or the RMS variation from the mean, and in frequency-domain as the LFSD (Low Frequency Sinusoidal Disturbance) which is the corresponding THD but for a DC system.

Transforming the results of the Fourier transform (or of the STFT) in dB μ V it is possible to compare the amplitude of each harmonic at different frequencies

in the range 2-150kHz with some proposed standard of emission as EN50065, CISPR 14&15, EN50160.

In an electrical system is not important only the maximum amplitude of a disturbance or a maximum amplitude of a harmonic, but it might be useful to consider with which probability the disturbance signals reach that amplitude. This is important because the designs of cables for HVDC lines are done taking into account the probability or the risk of breaking of the insulation at different disturbances considering also the probability that these disturbances occur. For electronic devices or digital transmission lines positioned near DC-lines linked with disturbance generators, it might be important, too. Amplitude Probability Distribution (APD) is a method to calculate the cumulative probability that a disturbance can exceed a certain value.

All these measuring methods and elaborations of real measured signals can be applied to simulation signals. In fact, using the extension of Matlab named Simulink, it is possible to simulate the configuration used for the real measurement and then apply the same algorithms to calculate PQ parameters and the harmonic amplitudes. This process might be a way to estimate the disturbances that devices as converters can generate, before these are linked to the line, or to estimate disturbances if LISN and others receivers are not available.

Chapter 1

DC SYSTEMS

While years ago DC distribution systems had been abandoned because the advantages of the AC distribution, mainly for the possibility to use transformer to change the voltage level for high distance transmissions, in the latest years, DC systems have been growing up. The reasons of this revenge of DC connections are more than one: the birth and the spread of distributed renewable generation, as solar or wind farms, of DC load, especially residential load, the necessity of storage electrical energy, the development of DC-DC converters and DC transmission cables. This set of devices, often, has to be connected to the AC network, too, so AC/DC converters have to be used. All these converters can be source of disturbance for the AC network or for the DC systems, too.

1.1 DC-Microgrid

A DC-microgrid, as shown in Fig.1, is a set of DC and AC generators, energy storage systems, DC loads and converters, all connected in a DC network at the same voltage level, or different ones through converters.

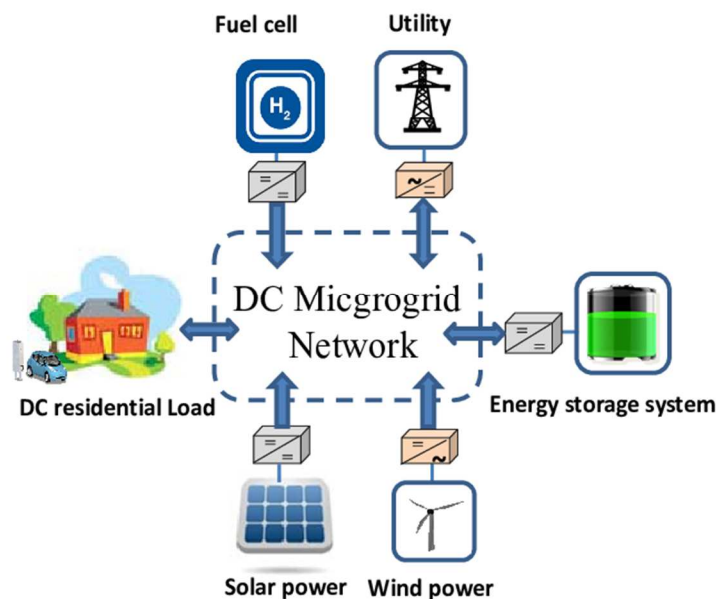


Figure 1

The main DC generators are solar power cells, positioned in the roofs of the buildings, for low power like some kW, or, for higher power like some megawatt, in open field. The energy production and the voltage level generated by these devices depends on the weather and change in the different hours of the day, so DC-DC converters are necessary to connect them to the microgrid to maintain its voltage level and to control the power flow. The same thing is possible to say if wind-farms are considered, again strongly dependent on weather conditions. Furthermore, the wind generators produce AC power, so, if they have to be connected to a DC network, AC/DC converters are necessary, to control the flow power, too.

As already said, these renewable energy productions cannot be programmed but only, with weather forecasts, expected. To optimize the utilization of this kind of energy, energy storage systems have to be installed. In fact, when the weather conditions allow the renewable generators to produce more power than it is requested, the systems continue to work in points of maximum production (MPPT algorithms) and the energy not requested is storage in these systems. Then, when weather conditions are worse for power production that becomes lower than the power requested, storage energy is used. The main storage energy systems are chemical batteries, which, in the last years with the development of the Li-ion battery, are becoming more and more used for these purposes. These storage devices have to be connected to the microgrid with DC-DC converter to control the voltage level and the power flows.

Other devices that are becoming more used not only in production of electrical energy, but also in storage energy, are the fuel cells. In fact, as the chemical batteries convert electrical energy to chemical energy and vice versa, they can use the Hydrogen generated by electrolysis using electrical energy, when the power requested is lower than the one produced by the renewable production systems, as fuel of the cells to product electrical energy when power requested is higher than the power generated. These cells have to be connected to the DC-microgrid with converters, too.

If all these energy production systems and energy storage systems have to feed only loads connected directly to the DC-microgrid, this rig is named “stand-alone”. In this case, production and storage energy have to be dimensioned correctly to have always-available power. Example of DC loads are electrical

residential and industrial devices designed to be supplied with DC power, electrical and industrial devices designed to be supplied with AC power (connected with an AC/DC converter), and electrical vehicles. Electrical vehicles, in a smart a large vision of renewable energy exploitation, can be seen not only as loads but as energy storage systems, too.

Often, a DC-microgrid is connected to the external network, too, because devices in that microgrid cannot be supplied by only energy production system within it and so it is necessary an external supply, or because when you want to transmit the excessive energy produced by renewable energy systems. In these cases, it is possible to connect the DC-microgrid to the main external network with an AC line, using an AC/DC converter between them, or with a DC line if high powers and long distances are requested.

Some of the advantages in the implementation of DC-microgrid are:

- higher efficiency and reduced losses due to the reduction of multiple converters used for dc loads;
- easier integration of various DC Distributed Energy Resources (DER), such as energy storage, solar photovoltaic (PV), and fuel cells, to the common bus with simplified interfaces;
- more efficient supply of dc loads, such as electric vehicles and LED lights;
- eliminating the need for synchronizing generators, which enables rotary generating units to operate at their own optimum speed;
- enabling bus ties to be operated without the need for synchronizing the buses.

These benefits, combined with the significant increase in electrical vehicles research and dc loads such as personal computers, laptop computers, LED lights, data and telecommunication centres have been encouraging research in DC microgrids.

On the other hand, the system integration of PV arrays, fuel cells, and batteries has some difficulties and requires some precautions: firstly, at least one of the converters must guarantee DC bus voltage regulation in any mode of operation. Secondly, power generation steps or other types of disturbances can affect system stability. Finally, the designed energy storage must contribute to system reliability and flexibility without discharging yourself completely.

Microgrid deployments have the purposes to:

- improve power quality;
- reduce emissions;
- reduce network congestion;
- reduce power losses;
- increase energy efficiency;
- improve system economics;
- islanding capability in the event of faults or disturbances in upstream networks, enhancing grid and customers' reliability and resilience.

AC-microgrids are associated to several problems as the need for synchronization of the distributed generators, inrush currents due to transformers, reactive-power flow, harmonic currents, and three-phase unbalances voltages. DC-microgrids could offer several advantages compared to AC-microgrids: providing a more efficient supply of dc loads by reducing losses due to the reduction of multiple converters used for dc loads, easier integration of DC DERs, and eliminating the need for synchronizing generators.

1.2 HVDC (High Voltage Direct Current)

Since when the couple pro-AC, Tesla-Westinghouse, got the better to Edison, pro-DC, at the end of the nineteenth century, AC generators, transmissions, distribution and utilization systems dominated the electric transmission world. This because the AC voltage conversion system was very simple, as transformers (with high nominal power and insulation, low losses and little maintenance), and 3-phase synchronous generators with power production higher than DC generators. The possibility to change AC voltage level for long transmission, thanks to transformers, permitted to extend the length of the transmission lines and so to build production centres far away to the cities or to exploit energy generation points which could not be near the main centres of utilization (for example hydroelectric generators).

Until the global electric network was a set of divided county or country networks, and the power requested by the loads, industrial and residential, there was no doubt about the supremacy of AC systems against DC systems. When electric network configuration started to change, AC power transmission disadvantages appeared. There are AC electric networks that working at

different frequencies cannot be connected, connections between independent AC systems are weak with the possibility of instability (Domino Effect) or undesirable power flows. The main problem is given by transmission line inductive and especially capacitive elements, which limit strongly the power capacity and the distance lines, especially for cable lines. In fact, due to the presence of high eddy capacitance p.u.l. along the entire line and high voltage level, active power P is not the only power transmitted, but capacitive reactive power Q is transmitted, too, as formula (1):

$$Q = \omega CV^2 \quad (1)$$

where C is the total capacitance, high for long lines. If an optimized reactive compensation is not done, this eddy reactive power request limit the active power and the length of the lines (40-120km).

All these problems and the development of converters permitted the spread of DC lines especially with high voltage levels: HVDC. In fact, as shown in figure 2, two AC networks can be connected with a DC line between them thanks the presence of AC/DC converters.



Figure 2

The low voltage level and high current level (high ohmic losses that cut down the transmittable power) problems that discouraged DC transmission, now disappear because new converters can bear high voltage levels. Overcoming these problems, DC transmission advantages come out:

- The presence of the only ohmic losses in conductor;
- No skin and proximity effect;
- No dielectric losses, presented only with variable voltages;
- No induced losses in sheath, armouring, neighbouring cables;
- No limitation of the length-current due to the eddy reactive power;
- Higher average electric field, higher cable utilization;

- Power flow easily and quickly controllable that improve AC system stability with DC links;
- Possibility to connect AC network at different frequencies (asynchronous link with almost no increase in fault level).

Low losses permit to have, for same power rating, HVDC cables (also extruded, easy to produce) cheaper than HVAC cables, saving conductor and insulation. Furthermore, to transmit the same power of an AC three cables system, a DC two cables system is used, having an even lower p.u.l. line cost.

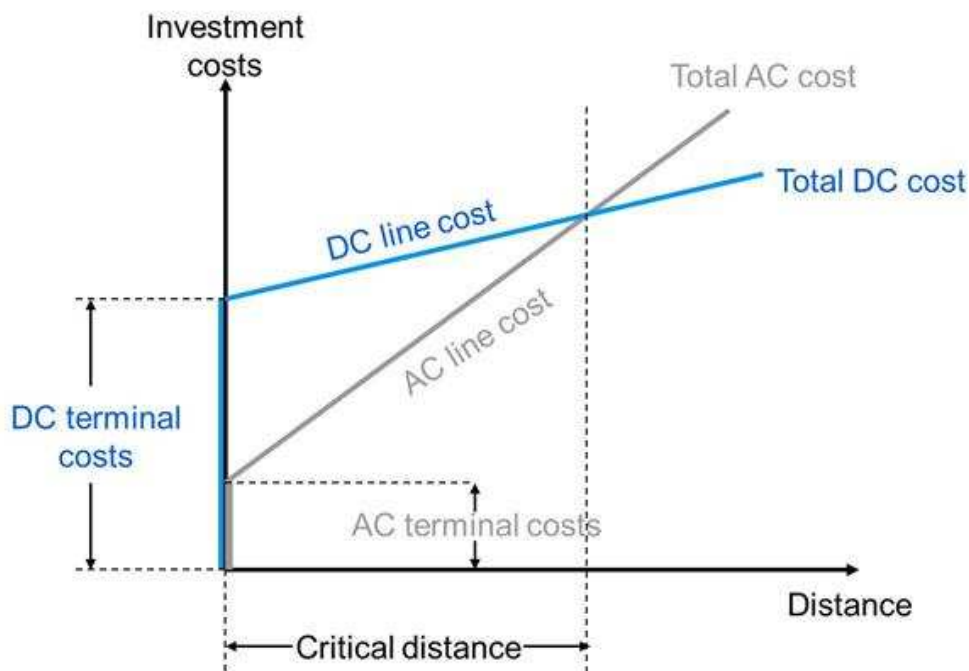


Figure 3

As shown in figure 3, the disadvantages of the DC transmission lines are the DC terminal costs, as converter transformer and converters, while in AC systems, transformers are cheaper thanks to an easier manufacture and a consolidated technology. As said above, the advantages of DC transmission are the lower DC line cost than the AC one, so, HVDC becomes interesting when the transmission distance becomes long enough to compensate terminal costs with lower line costs; the distance when the total AC cost reaches the total DC cost is named Critical Distance or Break-Even Distance.

Generally, the power of an HVDC transmission system is over 100 MW and is usually between 1000 and 3000 MW. The most HVDC lines now in function are collocated under the sea, linking mostly different countries. For example

the 580km NorNed cable between Norway and the Netherlands, Italy's 420km SAPEI cable between Sardinia and the mainland, the 290km Basslink between the Australian mainland and Tasmania, and the 250 km Baltic Cable between Sweden and Germany.

Tough with HVDC the problem of power losses is overcome for medium distance transmission ($\approx 150\text{km}$), this problem comes back when the length is even longer and the power transmitted increases. The way to overcome this problem is to increase more the voltage level. Doing that on such lines reduces the power loss, but until recently, the inter-connectors required to bridge the segments were prohibitively expensive. However, with advances in manufacturing, it is becoming more and more feasible to build the UHVDC lines (DC voltage transmission of at least 800kV). In 2010 ABB Group built the world's first 800kV UHVDC transmission line between Xiangjiaba and Shanghai China. The line crosses a total length of 1907km (1192mi). Since the Xiangjiaba-Shanghai line was completed in 2010, at least twelve other Chinese UHVDC transmission lines have been completed and about five more are still under construction. Some of the completed lines run at 1 million volts and span 2500km. Lines up to 5000km are currently being planned. In July 2016, ABB Group received a contract in China to build an ultra-high-voltage direct-current (UHVDC) land link with a 1100 kV voltage, a 3,000 km (1,900 mi) length and 12 GW of power, setting world records for highest voltage, longest distance and largest transmission capacity.

Chapter 2

CONVERTERS

With the increasing number of different ways to produce electric energy and different electric loads, the necessity of conversion from each kind of transmission has become more requested, too. Electric energy by fossil energy and wind energy is mainly produced in alternative mode due to the 3-phase synchronous generators used for this purpose; instead, the electric energy by photovoltaic cells or fuel cells is produced in direct mode. All these different types of power have to flow in the same grid, small or big, thus have to be transmitted in the same mode. At the load side, wide topology of utilization of electricity is present: from high power industrial 3-phase inductive motors, to small DC devices with different voltage levels. The increasing of DC smart grids, due to the renewable distribution energy production, asks the manager of the electric network an even greater development of the production and transmission control systems. The usage of converters has become more and more common in the last years. AC to DC converters, as rectifiers uncontrolled or controlled, or switching, DC to AC converters, as inverters, and DC to DC converters, as Buck or Boost converters, have been developed to improve life, behaviour and voltage and current performances. The research in this branch of electronic and electrical engineering permitted to optimize the dimensions of these devices and their functioning: the elements of the converters became smaller and resistant to higher electrical forces.

Inverters, DC/DC converters and AC to DC switching converters functioning is based on the commutation of static switches to obtain an “on-off” regulation of the quantities (current or voltage). The switching frequency of the converter is a characteristic of them and, to obtain output quantities that follow the requested signal, is higher than kHz.

The negative side of the connection of all these converters at the network is the decreasing of the Power Quality (PQ), which can worsen the devices functioning and even damage them. In fact, converters produce disturbance signals due to how they work, signals at different frequencies than the 50Hz (or 60Hz in America), especially at higher frequency as their switching frequency,

with amplitudes which sometimes cannot be neglected. Obviously, if the output of a converter is DC, the only component requested, ideally, is the 0Hz one, but, for the reason said above, in this case disturbances at high frequencies will be present, too.

2.1 DC/DC Converters-Buck Converter

As already said, converters are useful not only to change the electric transmission modes from AC to DC or vice versa, but they are used also to change voltage and current levels in the same Direct mode, as AC transformers do, with different principles, for alternative mode. This kind of converters are named DC/DC converters. There are two types of DC/DC converters: linear converters and switching converters.

The linear converters are circuits that exploit an internal reference and adjust the output voltage with an internal feedback. Being linear circuits, output voltage is always lower than the input voltage. The quantity $V_{in}-V_{out}$ is called “drop-out” and the minimum drop-out limits the minimum input voltage that permit the functioning of the circuit and maintain the adjusted output. Though they are less noisy and have an output really accurate (some per cent, better than switching converters), they are less flexible than switching converters and have low efficiency and high power losses that depend on the difference $V_{in}-V_{out}$.

The most of the switching converters are circuits that exploit the principle of the Pulse Width Modulation (PWM), but they have the possibility to have at the output a higher voltage level than the input, and not only lower, changing the position of the converter elements. There are Buck converters that can only give a lower output voltage, Boost converters that give higher output voltage, combinations of these two, Buck-Boost converters, which can give lower and higher output voltage than the input, and other configurations. Usually they apply a direct voltage to an inductor for a period of time, turning on the switch, during which a current flows storing magnetic energy that is transferred at the output when the switch is turned off. This is a really efficiency way of conversion but is more noisy for the switching functioning.

Buck converter

A Buck converter is a DC/DC switching converter step-down, thus, the output voltage can never be higher than the input voltage. The circuit is shown in figure 4, where a switch, a diode, an inductor and a capacitor are present.

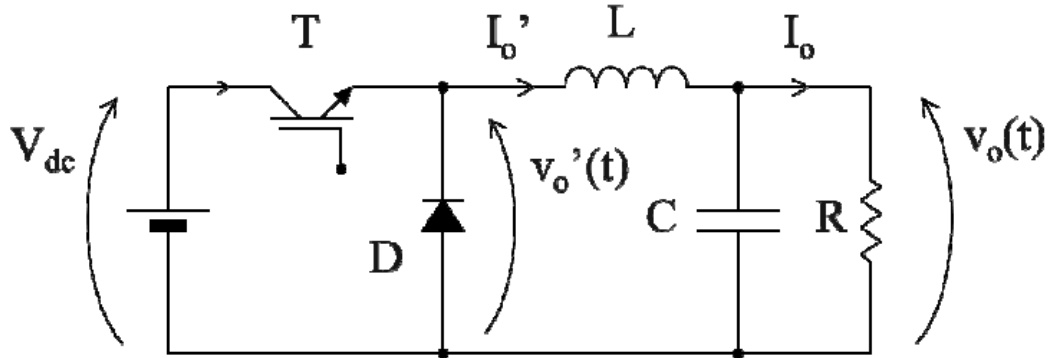


Figure 4

As said above for switching converters, to have different voltages at the output, duty cycle of the switch is changed.

To understand the functioning of this converter, it might be useful to study how current, voltage and power vary during a period T in the inductor and capacitor.

Inductor

For an inductor L we have:

$$v_L = L \frac{di_L}{dt} \quad (2)$$

Therefore:

$$i_L(t) - i_L(0) = \frac{1}{L} \int_0^t v_L(t) dt \quad (3)$$

If we work with periodic functions, inductor current at the start and at the end of the period is the same:

$$i_L(T) - i_L(0) = 0 \quad (4)$$

So:

$$i_L(T) - i_L(0) = \frac{1}{L} \int_0^T v_L(t) dt = 0 \quad (5)$$

If we split the period T in the period “on” and “off” of the switch:

$$\int_0^{t_{on}} v_L(t) dt + \int_{t_{on}}^T v_L(t) dt = 0 \quad (6)$$

Thus, the average inductor voltage value is:

$$\overline{v_L}(t) = V_L = 0 \quad (7)$$

Capacitor

For a capacitor C we have:

$$i_C = C \frac{dv_C}{dt} \quad (8)$$

Therefore:

$$v_C(t) - v_C(0) = \frac{1}{C} \int_0^t i_C(t) dt \quad (9)$$

If we work with periodic functions, capacitive voltage at the start and at the end of the period is the same:

$$v_C(T) - v_C(0) = 0 \quad (10)$$

So:

$$v_C(T) - v_C(0) = \frac{1}{C} \int_0^T i_C(t) dt = 0 \quad (11)$$

If we split the period T in the period “on” and “off” of the switch:

$$\int_0^{t_{on}} i_C(t) dt + \int_{t_{on}}^T i_C(t) dt = 0 \quad (12)$$

Thus, the average capacitor current value is:

$$\bar{i}_C(t) = I_C = 0 \quad (13)$$

Power

If we want to see if the input power is the same provided to the output, we have to do a power balancing of instantaneous powers:

$$p_i(t) = p_o(t) + \frac{d}{dt} W_L(t) + \frac{d}{dt} W_C(t) + p_d(t) \quad (14)$$

Where p_i is the input power, p_o is the output power, p_d is the loss power and:

$$W_L(t) = \frac{1}{2} L i_L^2 \quad (15)$$

$$W_C(t) = \frac{1}{2} C v_C^2 \quad (16)$$

If this balancing is done taking the average value of the quantities during a period T:

$$P_i = \bar{p}_i(t) = \bar{p}_o(t) + \frac{1}{T} \Delta W_L(0, T) + \frac{1}{T} \Delta W_C(0, T) + \bar{p}_d(t) = P_o + P_d \quad (17)$$

Neglecting the losses:

$$P_i = P_o \quad (18)$$

The study of the Buck converter is based on the observations above. As already said, the integral over the period T of the inductor voltage is equal to zero. We can split the integral in two stages: “on” when the switch is closed and “off”

when the switch is open. As shown in figure, in the stage “on”, during a period of time “ t_{on} ”, the voltage at the inductor is $(V_{DC} - V_o)$, while in the stage “off”, during the time “ $T-t_{on}$ ”, the voltage is “ $-V_o$ ”. Thus:

$$\int_0^T v_L(t)dt = (V_{DC} - V_o)t_{on} - V_o(T - t_{on}) = 0 \quad (19)$$

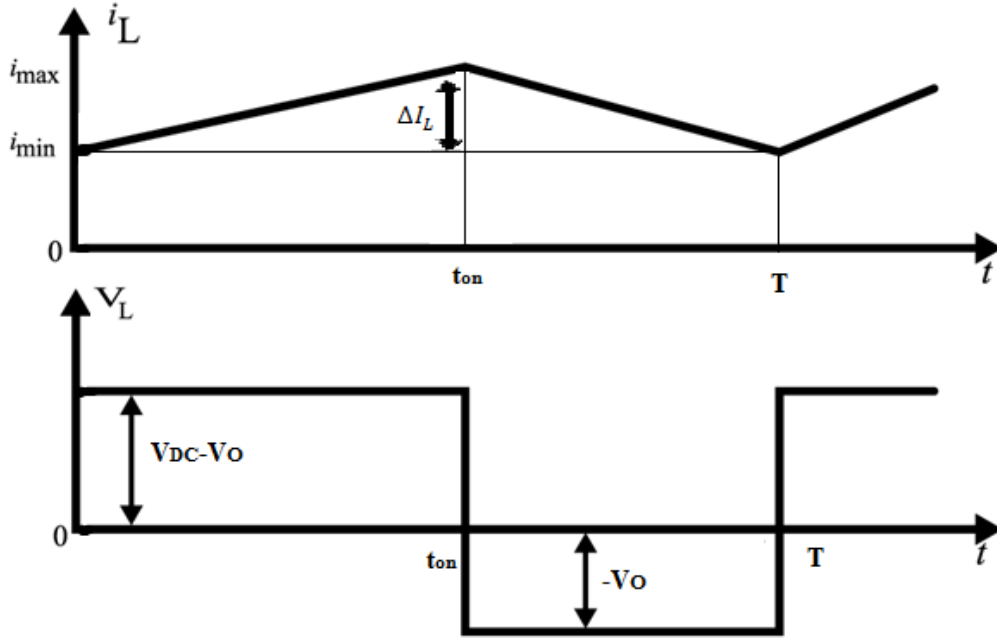


Figure 5

Dividing by the period T :

$$(V_{DC} - V_o)\delta - V_o(1 - \delta) = 0 \quad (20)$$

With:

$$\delta = \frac{t_{on}}{T} \quad \text{Duty Cycle.} \quad (21)$$

Elaborating the formula (20):

$$V_o = \delta V_{DC} \quad (22)$$

From the power balancing (18):

$$I_{DC} = \delta I_o \quad (23)$$

With:

$$I_o = \frac{V_o}{R} = \frac{\delta V_{DC}}{R} \quad (24)$$

And:

$$I_L = I'_o = I_o \quad (25)$$

because $I_C = 0$ from the propriety of the average capacitor current.

The value of the inductor is calculated from the variation of inductor current (variation assumed linear) that is:

$$\Delta I_L = \frac{(V_{DC} - V_o)}{L} t_{on} \quad (26)$$

Other currents to know for the thermal sizing of the components are:

$$I_T = \delta I_o = I_{DC} \quad \text{during } 0 - t_{on} \quad (27)$$

$$I_D = I_o(1 - \delta) \quad \text{during } t_{on} - T \quad (28)$$

Continuous and discontinuous mode:

The buck converter can operate in two different modes; continuous conduction mode (CCM) and discontinuous conduction mode (DCM). The difference between the two, shown in figure 6, is that in CCM the current in the inductor does not fall to zero.

A buck converter operates in continuous mode if the current through the inductor never falls to zero during the commutation cycle. In DCM, the current through the inductor falls to zero during part of the period.

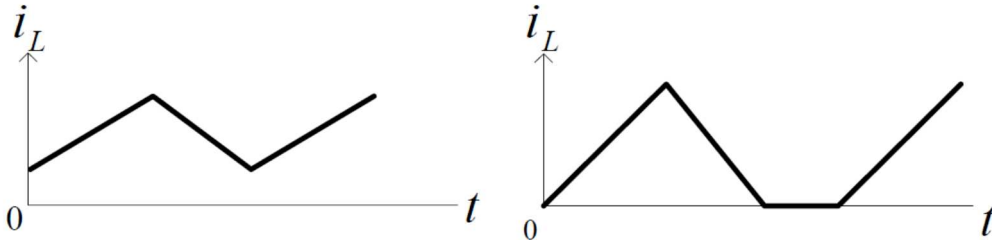


Figure 6

A condition determines the passage from continuous mode to discontinuous mode. To guarantee an uninterrupted flow of I_L through the inductor, the inductor has to be:

$$L > \frac{(1-\delta)}{2} TR \quad (29)$$

Or:

$$L > \frac{(1-\delta)}{2f} R \quad (30)$$

2.2 HVDC Converters

HVDC transmission requires AC/DC converters with, ideally:

- high power and voltage ratings;
- low losses;
- high reliability;
- acceptable costs;
- good performances.

Two types of converters are mainly used for DC transmission:

- Line-Commutated Current-Source Converters (LCC);
- Self-Commutated Voltage-Source Converters (VSC).

LCC converters were the first to be developed, from the firsts using mercury arc rectifiers in the 1930s, passing for the Silicon Controlled Rectifiers (SCR), and now at the state of the art with Light-Triggered Thyristors (LTT).

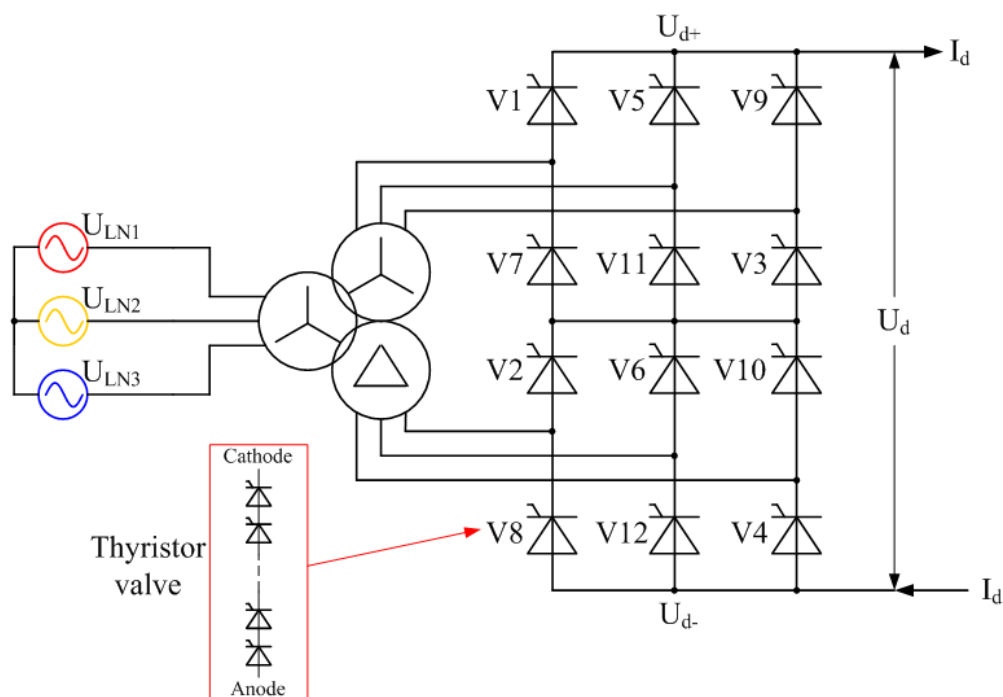


Figure 7

A 12-pulse HVDC converter using thyristor valves, shown in figure 7[11], is effectively two six-pulse bridges connected in series on the DC side and arranged with a phase displacement between their respective AC supplies so that some of the harmonic voltages and currents are cancelled. With twelve valves connecting each of the two sets of three phases to the two DC rails, there is a phase change every 30° , and harmonics are considerably reduced. For this

reason the twelve-pulse system has become standard on almost all line-commutated converter HVDC systems.

LTT have the highest power and voltage ratings and a high reliability. If power flow reversal is required, it is done reversing the voltage polarity, which is critical for HVDC extruded cable insulation. DC-LCC transmission solution has a very high transmission power and low cable and conversion losses, but it needs large space and, due to the injection of current and voltage harmonics, capacitor banks on AC side and harmonic filters on AC and DC side. LCC converters require reactive power from AC nodes, with an AC network that has to be strong.

VSC converters are more recent (late 1990s) than LCC. VSC converters use semiconductors with turn-off capability, as IGBT, which can re-turn on without the necessity of a network signal (good for distant lines). They work in four-quadrant operation, but they have high losses.

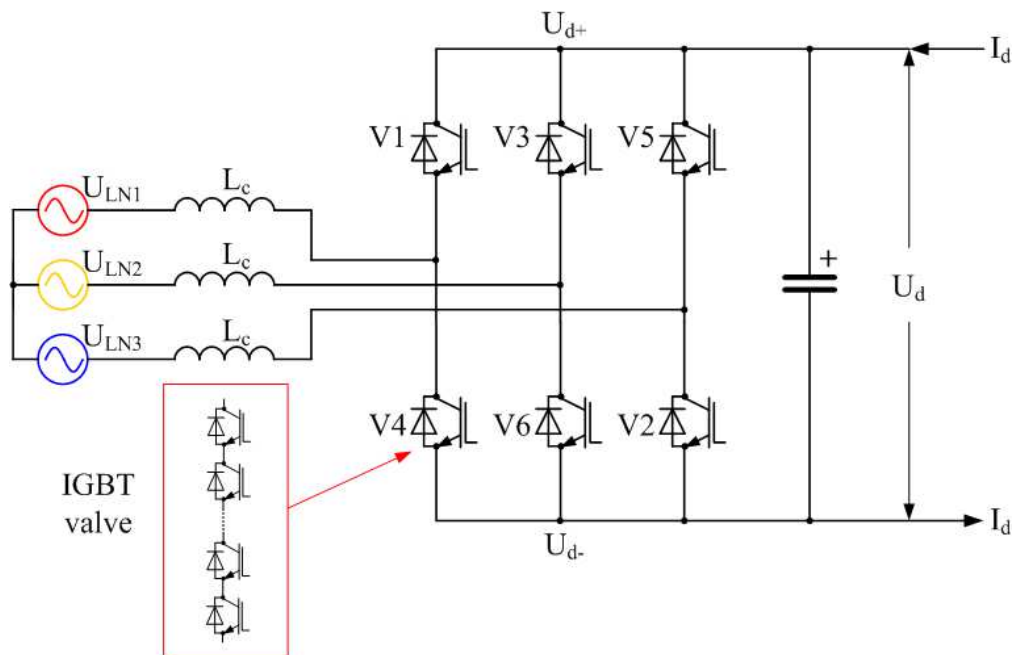


Figure 8

A three-phase, two-level voltage-source converter for HVDC is shown in figure 8[11].The simplest (and also, the highest-amplitude) waveform that can be produced by a two-level converter is a square wave; however this would produce unacceptable levels of harmonic distortion, so some form of Pulse-width modulation (PWM) is always used to improve the harmonic distortion of the converter. Because of the PWM, the IGBTs are switched on and off many times (typically 20) in each mains cycle. This results in high switching losses in

the IGBTs and reduces the overall transmission efficiency. Several different PWM strategies are possible for HVDC but in all cases, the efficiency of the two-level converter is significantly poorer than that of a LCC because of the higher switching losses. In an attempt to improve on the poor harmonic performance of the two-level converter, some HVDC systems have been built with “three level converters”, shown in figure 9[11].

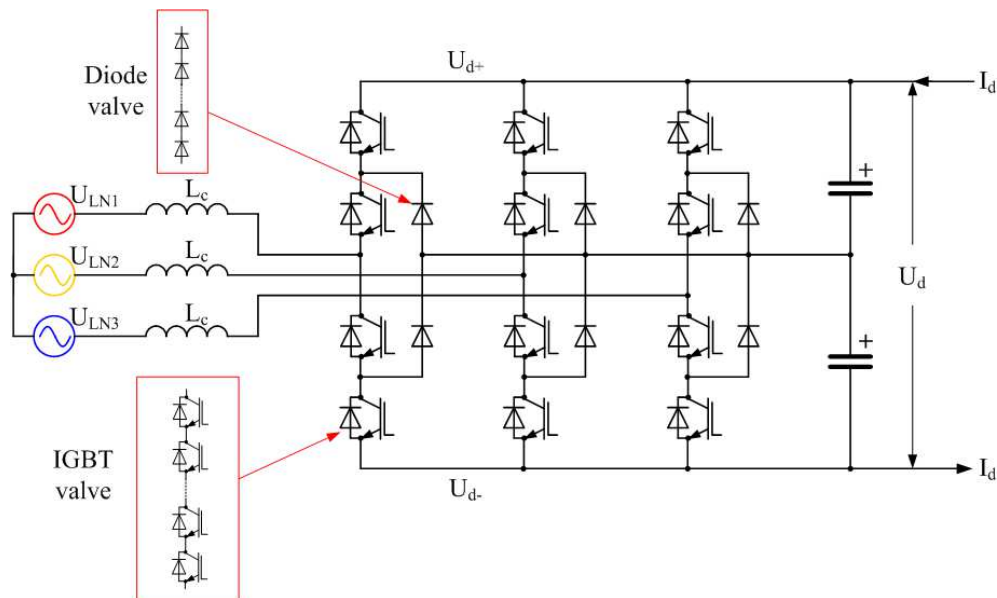


Figure 9

Three-level converters can synthesize three (instead of only two) discrete voltage levels at the AC terminal of each phase: $+\frac{1}{2} U_d$, 0 and $-\frac{1}{2} U_d$. To obtain a positive output voltage ($+\frac{1}{2} U_d$) the top two IGBT valves are turned on, to obtain a negative output voltage ($-\frac{1}{2} U_d$) the bottom two IGBT valves are turned on and to obtain zero output voltage the middle two IGBT valves are turned on. Unlike LCC converters, VSC do the power flow reversal by reversing the current flow, so, there are not critical situations for extruded cables. DC-VSC transmission solution can feed isolated loads as oil platforms, small island, wind parks, and needs small place, but VSC converters have limited voltage and power ratings, due mainly to a low experience.

The two main HVDC line configurations are: monopolar system and bipolar system.

The monopolar system is the cheapest and the simplest, used for moderate powers. It is made of two converters and only one high voltage pole. For the return current there alternatives:

- Ground/sea electrodes;
- A metallic return grounded at one converter station;
- Splitting a 12-pulse converter and grounded the midpoint.

The bipolar system is the most common, with one 12-pulse converter per pole and terminal, making two independent circuits with half capacity each. It can have different operating modes/configuration:

- Normal (balanced): with no ground current (Bipole);
- Monopolar ground return: if a cable is broken, current uses the ground return (Bipole);
- Opposite pole for metallic return: if a converter is broken, we change the configuration using switches to bypass it (Bipole, Metallic Return).

Chapter 3

MEASURING AND ELABORATION METHODS FOR CONDUCTED EMISSIONS WITHIN THE RANGE 2-150kHz

No-linear devices, as DC/DC and AC/DC switching converters, besides their own functions, due to how they work, generate disturbances that might worsen the behavior of others linked devices, and even damage themselves, too. In networks where there are connected renewable energy production stations, as DC microgrids, the presence of these types of devices is very common, and lately, with the increasing of this kind of production, they are increasing, too. Disturbances generated by these devices do not vary only in time or in amplitude, but they have a large variation along the frequency spectrum. This is mainly due to their switching functioning, which produces transients or periodic injections of signals with components at the switching frequency, at multiples of it, and sometimes at no-multiple frequencies. All these components are called harmonics and they can have different amplitudes and different effects; components that are transmitted to the other devices mainly through the cables of the network if the frequencies are not too high (until 30MHz). As will be discussed in Chapter 4, there are standards of Power Quality and standard limits for conducted emission, thus, to say if a device or a set of devices have these quality requirement, measuring and elaboration methods of these emitted disturbances have to be developed.

While for frequencies up to 2kHz and starting from 150kHz there are standards and normatives for these purposes, in the frequency range 2-150kHz there are only proposed methods and emission limits. Therefore, it might be interesting finding new methods for this range, or adapting methods of the other ranges. In the frequency range 150kHz-30MHz, to measure conducted emissions a LISN (Line Impedance Stabilization Network) is used, with the aim of standardizing the measuring process; to visualize the measured signals, an EMI receiver

(spectrum analyser) is used. Using the LISN to measure conducted emissions in the range 2-150kHz for a DC microgrid is one of the aims of thesis. If we want to elaborate the measured signals with an own processing program, it might be used an acquisition device connecting the signal port of the LISN to the acquisition system.

Once the signal is measured and sent to the laptop, it can be elaborated to achieve the desired conclusions. As already said, disturbance signals are combinations of harmonics at different frequencies, thus, a study in the frequency domain may be necessary. The theory of Fourier analysis says that a signal can be represented in a sum of sinusoids at different frequencies. Thus, in order to use the Fourier transform, to represent disturbances, is necessary to identify the amplitudes of the signals at the different frequencies.

Using MATLAB as the program to elaborate disturbance signals, the Fourier transform is replaced with the Fast Fourier Transform, which is an algorithm that makes faster the harmonic components calculation. Fourier Transform is used for steady-state signals, but in a microgrid, due to the presence of variable loads, generators and loads failures, and other events, there are electromagnetic transients. For this reason, a study of the disturbances not only in the frequency domain, but also in the time-frequency domain might be necessary. To achieve this purpose, Short Time Fourier Transform (STFT) is used, which splits the measured signal in more segments and then applies the FFT to each segment. In this way, we can have a view of how the harmonics and their amplitudes vary during the time.

Besides the time domain, frequency domain and time-frequency domain representation of the signals, a probabilistic study of disturbances has become more and more useful to understand the behaviour of electric networks and their design. For this aim, the calculation of the Amplitude Probability Distribution (APD) might be interesting.

3.1 Line Impedance Stabilization Network (LISN)

The necessity of comparing measurements of disturbances in different network conditions with electromagnetic compatibility standards, created the necessity

to have standard measurement devices and methods. For this purpose, Line Impedance Stabilization Network (LISN) has been developed. The LISN is designed to measure 50/60Hz devices conducted emissions in the frequency range 150kHz-30MHz. There are one-phase or three-phases LISN, but all follow the principles of the one-phase electric circuit represented in figure 10.

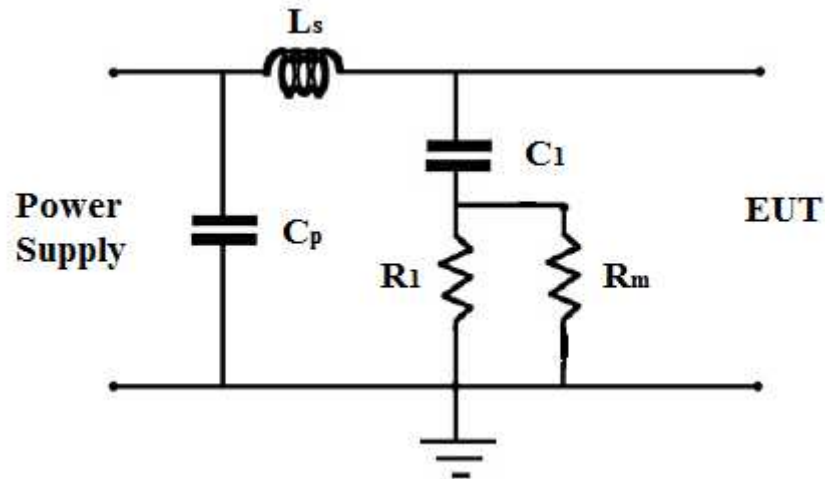


Figure 10

The LISN is positioned between the power supply and the Equipment Under Test (EUT), and, if we consider a one-phase measurement device, connected to the phase connector and the ground one. The third connection is for the receiver, represented with the resistance R_m . The aims of this circuit are more than one. First, being positioned between the supply and the device, it has to let pass the 50Hz current component for the device functioning. For this purpose, the series component L_s has to have a low impedance at 50Hz (is a short circuit for the DC component); an inductance of $50\mu\text{H}$, as shown in table 1, at 50Hz has an impedance of $15.7\text{m}\Omega$. The second aim of the LISN is to prevent that the disturbances that come from the external network could influence the measurement; this is achieved thanks to the shunt capacitance C_p , usually of $1\mu\text{F}$, which at frequencies between 150kHz and 30MHz has low impedance values, and the inductance L_s that, instead, has high impedance values at high frequencies. Capacitance C_p that at 50Hz has a high impedance, thus it does not filter the 50Hz component, too. At the opposite side, LISN has a series C_1 - R , which shunts the EUT. The capacitance C_1 , usually of $0.1\mu\text{F}$, has the purpose to filter the high frequencies coming from the EUT, closing them to the resistance R , usually of $1\text{k}\Omega$. This resistance is the one that is connected in parallel with the resistance R_m of the EMI receiver.

Table 1

Component	Z @50Hz	Z @2kHz	Z @150kHz	Z @30MHz
L=50 μ H	15.7m Ω	0.63m Ω	47.1m Ω	9.425k Ω
C=0.1 μ F	31.8k Ω	796 Ω	10.6 Ω	53m Ω
C=1 μ F	3.18k Ω	79.6 Ω	1.06 Ω	5.3m Ω

All these components and the 50 Ω resistance of the receiver let the LISN be an impedance stabilization network, letting us to have comparable results for every measurements. In fact, the supply network impedance may be really variable with the frequency (from few ohms, to hundreds ohms). The parallel between the R1 and Rm gives a constant impedance, for the high frequency disturbance signal, of about 50 Ω ; signal that is directed to the input of the receiver. The other components divide the power supply and the EUT at high frequency.

R1 has also a safety function: it lets discharge the capacitance C1 when the LISN is disconnected. It has a resistance comparable with human resistance; if it is higher, the discharge might take too much time and might occur through the human body.

Being born for 150kHz-30MHz conducted emission measurements, in the frequency range 2-150kHz some problems might arise. In fact, as table 1 shows, in this range, especially for low frequencies near 2kHz, the components assume values that can influence the measurements. Series inductance might let pass disturbances from the network to the EUT and the receiver, and vice versa; shunt capacitance Cp might not filter network disturbances; capacitance C1 might not let pass the disturbance signals from the EUT to the resistance R1 and, thus, to the receiver.

The measurement procedure starts with the positioning of the devices, preferably, as the normative says, as in the figure 11.

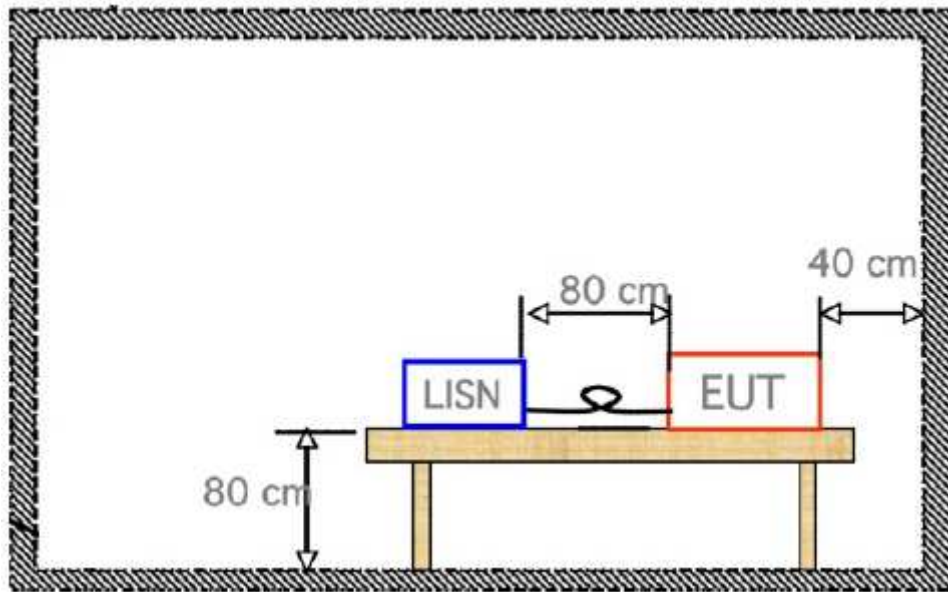


Figure 11

The table should be made with no-conductive material and long cables should be collected with shapes that decrease the coupling. It might be better if the measurements were done in a shielded room to decrease, even more, external influences. Once devices are connected, a first measurement, with the EUT off (but connected), should be done to know the network background noise. After that, a measurement, for every conductor, is done with the EMI receiver in the appropriate frequency range. When we are measuring the conducted emissions from, for example, the phase cable, the port of the LISN connected to the neutral cable has to be balanced with a 50Ω resistance.

3.2 Fourier Transform (FT)

The Fourier Transform (FT) is an integral transform, with several application in physics and engineering developed by the French mathematical Jean Baptiste Joseph Fourier.

It allows writing a time dependent function in the frequency domain, decomposing the function in the base of the exponential functions with a scalar product; the representation is called “spectrum of the function”. The Fourier Transform is invertible: from the transformed of a function is possible to go back to the function using the inversion theorem of Fourier.

If the function is periodic, the Fourier Transform can be simplified by the calculation of a discrete set of complex amplitudes, called “Fourier series coefficient”. The lowest frequency is called “fundamental harmonic” and it is the one with the highest weight for the final signal re-composition, while the other frequencies are multiply of the fundamental and they are called “secondary harmonics”.

If the signal has an average value different from zero, the Series gives also a component that represent it. If a periodic signal is cut at the external of a certain interval in abscissa staying defined only internally, the resulting spectrum will be the discrete one where, in each row, it is extended in the dependent variable dominion, with a value equal to the reverse of the definition signal interval.

If the function is not periodic, the spectrum is continuous, and it is the wider in the frequencies axis the more original domain of the independent variable is limited, and vice versa.

The Fourier transform of the function x is traditionally denoted by adding a circumflex symbol: \hat{x} . There are several common conventions for defining the Fourier transform of an integrable function $x: \mathbb{R} \rightarrow \mathbb{C}$. One of them is:

$$\hat{x}(f) = \int_{-\infty}^{+\infty} x(t)e^{-2\pi itf} dt \quad (31)$$

for any real number f .

The independent variable t represents time, the transform variable f represents frequency (e.g. if time is measured in seconds, then the frequency is in hertz). Under suitable conditions, x is determined by \hat{x} via the inverse transform:

$$x(t) = \int_{-\infty}^{+\infty} \hat{x}(f)e^{2\pi itf} df \quad (32)$$

for any real number t .

Fourier Series

Every periodic signal of period T can be represented as a sum of infinite terms having sinusoidal trend by the Fourier Series:

$$x(t) = X_0 + \sum_{h=1}^{\infty} X_h \cos(h\omega_1 t + \varphi_h) \quad (33)$$

Being ω_1 defined with the period of the signal as:

$$\omega_1 = \frac{2\pi}{T} \quad (34)$$

Results:

$$x(t) = X_0 + \sum_{h=1}^{\infty} X_h \cos\left(\frac{2\pi}{T} ht + \varphi_h\right) \quad (35)$$

Generally, $x(t)$, $t \in [0, T]$ is called representation of the signal x in the time domain, while, in the form (33), the representation in the frequency domain $\{(X_h, \varphi_h) \ h=0,1,\dots\}$ is used, called signal spectrum.

The sinusoidal or co-sinusoidal terms are called “signal harmonics” and they are characterized of the harmonics order “ h ”, the ratio between their pulsation and the pulsation ω_1 :

$$h_i = \frac{\omega_i}{\omega_1} \quad (36)$$

Alternately, the harmonic of h order can be decomposed in two terms with same pulsation and 90° out of phase, using the trigonometric identity:

$$\cos(a + b) = \cos(a)\cos(b) - \sin(a)\sin(b) \quad (37)$$

modifying (33):

$$X_h \cos(h\omega_i t + \varphi_h) = X_h \cos(\varphi_h) \cos(h\omega_i t) - X_h \sin(\varphi_h) \sin(h\omega_i t) = A_h \cos(h\omega_i t) + B_h \sin(h\omega_i t) \quad (38)$$

The coefficients of the Fourier Series decomposition of a periodic signal $x(t)$ of period T can be calculated by integration with the equations:

$$X_0 = \frac{1}{T} \int_{-T/2}^{T/2} x(\omega t) d(\omega t) \quad (39a)$$

$$A_h = \frac{2}{T} \int_0^T x(\omega t) \cos(h\omega_1 t) d(\omega t) \quad (39b)$$

$$B_h = \frac{2}{T} \int_0^T x(\omega t) \sin(h\omega_1 t) d(\omega t) \quad (39c)$$

Discrete Fourier Transform (DFT) and Fast Fourier Transform (FFT)

The Fourier analysis, when applied to a continuous periodic signal in the time domain, produce a series of component of discrete frequency in the frequency domain.

If the case the spectrum in the frequency domain, as in the time domain, is a sampled function, the Fourier Transform is composed of discrete components:

$$X(f_k) = \frac{1}{N} \sum_{n=0}^{N-1} x(t_n) e^{-i2\pi kn/N} \quad (40)$$

And the anti-transformer is:

$$x(t_n) = \frac{1}{N} \sum_{k=0}^{N-1} X(f_k) e^{i2\pi kn/N} \quad (41)$$

In conclusion the Discrete Fourier Transform is obtained sampling the function $x(t)$ and doing the integer numerically of the equations (39).

Having:

- N the number of the samples;
- Δ the sample period, the interval between one sample and the next one (expressed using the electric angle in radian):

$$\Delta = \frac{2\pi}{N} \quad (42)$$

The generic k sample x_k of the function $x(t)$ is expressible with:

$$x(\omega t) = x(k\Delta) \approx x_k \quad \text{with } k=0,1,\dots,N$$

Therefore:

$$A_h = \frac{2}{T} \int_0^T x(\omega t) \cos(h\omega_1 t) d(\omega t) \approx \frac{2}{N} \sum_{k=0}^N x_k \cos(hk\Delta) \quad (43a)$$

$$B_h = \frac{2}{T} \int_0^T x(\omega t) \sin(h\omega_1 t) d(\omega t) \approx \frac{2}{N} \sum_{k=0}^N x_k \sin(hk\Delta) \quad (43b)$$

Fast Fourier Transform (FFT)

As seen, the DFT algorithm is a numeric approximation of the Fourier Transform, which transforms the terms of a time-sampled signal in a frequency spectrum. This transformation needs to carry out a large number of arithmetic operations. Only the multiplication to transform N sampling in $N/2$ frequencies

are N^2 , and due to the fact that to have a good definition it is required an N really high (for the Shannon Theorem), the time required to do that may be a limit for the practical applications.

A really improvement may be obtained applying a procedure known as Fast Fourier Transform (FFT), which delete the repetition of redundant multiplications, making the execution faster. The FFT is not an approximation of the DFT but it gives the same results, carrying out only $(N/2) \cdot \log_2(N)$ multiplications for (43). The advantage is higher, the higher is N : precisely the ratio of the multiplication required from the FFT and the ones required from the DFT is $\log_2(N)/(2N)$. The only limit of the of the FFT is the number of sampling that has to be an exact power of 2.

The result of the FFT of the sampled data vector \mathbf{x} of $x(t)$, is normally a vector of N complex numbers, \mathbf{X} . The structure of \mathbf{X} , for certain values of k and referring to the equations (43) is:

- $k=0$: continuous component of the sampled signal \mathbf{x} , multiplied per N .
- $k=1, \dots, N/2$: complex numbers that represent the harmonics of the sample signal \mathbf{x} , multiplied per $N/2$.
- $k=N/2+1, \dots, N$: same numbers obtained for per $k=1, \dots, N/2$, but placed in inverse order and conjugate complex.

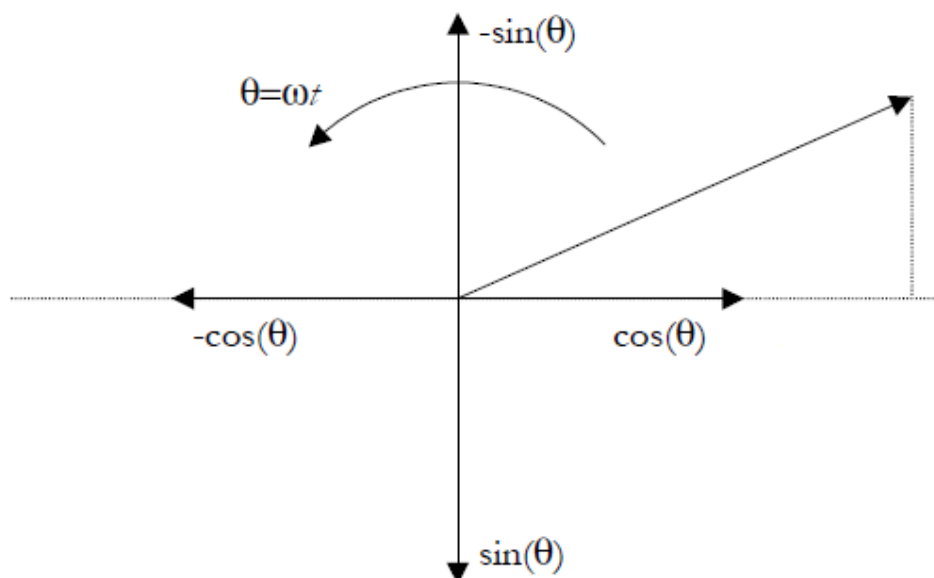


Figure 12

The sign of the terms of the FFT output is assigned using as reference the projections of the rotating vectors (anticlockwise) in the real axis.

Cooley–Tukey algorithm

The most commonly used FFT is the Cooley–Tukey algorithm. This is a divide and conquer algorithm that recursively breaks down a DFT of any composite size $N = N_1N_2$ into many smaller DFTs of sizes N_1 and N_2 , along with N multiplications by complex roots of unity traditionally called twiddle factors (after Gentleman and Sande, 1966).

The best known use of the Cooley–Tukey algorithm is to divide the transform into two pieces of size $N/2$ at each step, and is therefore limited to power-of-two sizes, but any factorization can be used in general (as was known to both Gauss and Cooley/Tukey). These are called the radix-2 and mixed-radix cases, respectively (and other variants such as the split-radix FFT have their own names as well). Although the basic idea is recursive, most traditional implementations rearrange the algorithm to avoid explicit recursion. Also, because the Cooley–Tukey algorithm breaks the DFT into smaller DFTs, it can be combined arbitrarily with any other algorithm for the DFT.

Aliasing

The aliasing, or distortion for slow sampling, or subsampling, in electronic is the phenomenon for which two different analogic signals may become indistinguishable when sampled for the slowness of the sampling: this is a real problem for the system output.

For example, when we want to find frequencies of periodic sampled signals, it may happen that the sampling transforms the Base Band of frequencies, characteristic of the original signal, in a series of bands that, overlapping and therefore interfering with each other, introduces false frequencies, called “ghost frequencies”.

When an observation of a phenomenon, whose band might reach a frequency F_s is required, a sampling frequency $F_c > 2F_s$, and thus an interval between the single observations, are necessary. This results is called Theorem of Shannon or Nyquists. Sampling at a frequency at least double of the max signal frequency, the ghost frequencies will not arise.

Converters as harmonic distortion sources

The harmonics in the electric networks are generated by the flux of the distorted currents within the network. The voltage harmonic distortion arises when, in the network, harmonic currents start to flow generating voltage drops in the equivalent impedance. The distorting devices produce and absorb harmonic distorted current. The static converters, DC/DC, AC/DC, DC/AC, are an example of polluting loads. In fact, the harmonic order of the static converter AC/DC is expressed by:

$$h = mq \pm 1 \quad (44)$$

where q is the number of the converter impulses and m is a positive integer number. Thus, for example, for a six-pulse converter, the characteristic harmonics are the 5th, 7th, 11th, 13th and so on.

Ideally, the amplitude of each harmonic component is proportional to $1/h$, with h the harmonic order.

3.3 Short Time Fourier Transform (STFT)

As already said, in an electric network there are not only periodic disturbances, but also transient ones. These disturbances have amplitudes and harmonic components that change during the time. For these reasons the simple Fourier Transform, with its algorithms, is not sufficient anymore for the disturbances studies. A time-frequency domain study is necessary for this purpose, using the Short Time Fourier Transform (STFT).

The Short Time Fourier Transform is a Fourier transform used to determine the sinusoidal frequency and phase content of local sections of a signal as it changes over time. In practice, the procedure for computing STFTs is to divide a longer time signal into shorter segments of equal length and then compute the Fourier transform separately on each shorter segment. This reveals the Fourier spectrum on each shorter segment. One then usually plots the changing spectra as a function of time.

Continuous-time STFT

Simply, in the continuous-time case, the function to be transformed is multiplied by a window function, which is nonzero for only a short period of time. The Fourier transform (a one-dimensional function) of the resulting signal is

taken as the window is slid along the time axis, resulting in a two-dimensional representation of the signal. Mathematically, this is written as:

$$STFT\{x(t)\}(\tau, \omega) \equiv X(\tau, \omega) = \int_{-\infty}^{+\infty} x(t)w(t - \tau)e^{-j\omega t} dt \quad (45)$$

where $w(t)$ is the window function, commonly a Hann window or Gaussian window centred around zero, and $x(t)$ is the signal to be transformed. $X(\tau, \omega)$ is essentially the Fourier Transform of $x(t)w(t-\tau)$, a complex function representing the phase and magnitude of the signal over time and frequency. Often phase unwrapping is employed along either or both the time axis, τ , and frequency axis, ω , to suppress any jump discontinuity of the phase result of the STFT. The time index τ is normally considered to be "slow" time and usually not expressed in as high resolution as time t .

Discrete-time STFT

In the discrete time case, the data to be transformed could be broken up into chunks or frames (which usually overlap each other, to reduce artefacts at the boundary). Each chunk is Fourier transformed, and the complex result is added to a matrix, which records magnitude and phase for each point in time and frequency. This can be expressed as:

$$STFT\{x[n]\}(m, \omega) \equiv X(m, \omega) = \sum_{n=-\infty}^{+\infty} x[n]w[n - m]e^{-j\omega n} \quad (46)$$

likewise, with signal $x[n]$ and window $w[n]$. In this case, m is discrete and ω is continuous, but in most typical applications the STFT is performed on a computer using the Fast Fourier Transform, so both variables are discrete and quantized.

STFT issues

Harmonic distortions are typically handled in this manner but for the analysis of inter-harmonics, non-linearity and non-stationarity, STFT faced difficulties because of constraint in frequency resolution. One of the pitfalls of the STFT is that it has a fixed resolution. The width of the windowing function relates to how the signal is represented; it determines whether there is good frequency resolution (frequency components close together can be separated) or good time resolution (the time at which frequencies change). A wide window gives better frequency resolution but poor time resolution. A narrower window gives good

time resolution but poor frequency resolution. These are called narrowband and wideband transforms, respectively.

Another method could be Wavelet transform (WT) which is increasingly being used to overcome the above difficulties. The advantage of using WT is that it does not need to assume the stationarity or periodicity of signals, not even within the analysis window. WT breaks the signal into multiple frequency bands, instead of a discrete number of frequency components as in FT.

3.4 Amplitude Probability Distribution (APD)

Besides disturbance studies in time domain, frequency domain and time-frequency domain, a probabilistic view of the conducted emission generators behaviour might be significant for the possible answer of the network and other linked devices. In fact, converters can be generators of overvoltage or overcurrent, with different frequencies and amplitude. Furthermore, these disturbance signals might resonance with other network devices amplifying the disturbances. Designs of HVDC cables and other devices are not done in a deterministic way, but statistically, with regard to the probability of their breakup to a certain disturbance, and the probability that this disturbance occurs. For these purposes, another way to evaluate the disturbance is calculating the APD, Amplitude Probability Distribution, born to estimate the bit-error-rate of digital communication system in the presence of electromagnetic interferences. The APD represents the probability that the interference has a certain value of amplitude or larger.

IQ Capture and DCS Simulation Procedure

This methodology is based on the in-phase and quadrature (IQ) components acquisition of the radiated interference in the frequency band of the communication system. Afterward, a simulation of the DCS (Digital Communication System) adding the interference previously measured is performed to determine the degradation produced by the impulsive noise.

Concerning the setup of the time-domain measurement, in the transient acquisition, the measurement instrument is connected to the electromagnetic

interference (EMI) receiver, which is centred in the working frequency of the DCS. The analogical input stage of the EMI receiver is used to filter the transient interference in the communication frequency band and down converts it to the intermediate frequency (IF). The IF output of the EMI receiver is connected to the input of the oscilloscope, which performs the tasks to detect transient events employing the trigger and also to store the IF transient interference described by the following equation:

$$x[n] = A_{IF} \sin(2\pi f_{IF}(n) + \varphi_{IF}) \quad (47)$$

where $x[n]$ is the discrete input signal modulated in the f_{IF} frequency, where $n = k\Delta t$. As an example, the IF of the EMI receiver used in these measurements is 20.4 MHz. The IF signal is obtained, setting the most accurate resolution bandwidth (RBW) from the available ones in the EMI receiver. The RBW, which shall be selected by the user, must be larger than the bandwidth of the real time communication systems. Once the IF signal has been acquired, the measurement methodology is able to compute the IQ components of the interference employing the mathematical software. First, the data are bandpass filtered in the IF centre frequency to avoid undesired spurious components. Second, the signal is demodulated obtaining the IQ components according to the following equations:

$$i[n] = x[n] \cos(2\pi f_{IF}(n)) \quad (48a)$$

$$q[n] = x[n] \sin(2\pi f_{IF}(n)) \quad (48b)$$

Afterward, $i[n]$ and $q[n]$, components of the interference are filtered with a low-pass finite impulse response filter equal to the RBW of the communication system.

It is essential to measure the APD employing the bandwidth of the system that is going to be evaluated. In this situation, the envelope detection is reached by means of the Hilbert Transform, which is used extensively for analysis and signal processing in passband communication systems. Otherwise, the envelope of the radiated transient interference can be obtained from the IQ components obtained in the post-processing stage as [4]:

$$r[n] = \sqrt{i[n]^2 + q[n]^2} \quad (49)$$

and the relation between $APD_R(r)$ and the probability density function (pdf) of the envelope R is

$$APD_R(r) = 1 - F_R(r) \quad (50)$$

And

$$f_R(r) = \frac{d}{dr} F_R(r) = -\frac{d}{dr} APD_R(r) \quad (51)$$

where $F_R(r)$ is the cumulative distribution function (cdf) and $f_R(r)$ is the pdf. The cdf describes the probability that a value of the envelope variable R with a given pdf will be found to have a value less than or equal to r . Finally, the APD is directly obtained from the cdf using the expressions shown above.

One of the main limitations is that measurement can only be performed with the pre-set filters available at the EMI receiver, which sometimes are different from the communication bandwidths causing an incorrect estimation on the degradation produced. Another restriction is the elapsed time needed to acquire the statistical APD measurement at each frequency band [6].

The goal is to obtain the APD measurements from time-domain captures. To achieve this, a mathematical software is employed. For this purpose Matlab might be used in order to filter the time-domain signal to get only the interference at the desired frequency band that it is going to be evaluated; the post-processing tool will also permit us to demodulate the interference in-phase and quadrature as receivers do; and, at the end, to perform an histogram of the measured amplitude to compute the amplitude probability distribution [5]. It is important to highlight that with the oscilloscope, one time-domain capture is valid to obtain the APD diagram at all desired frequency bands; post-processing tools are suitable to manage the same input data to get the APD diagram at the frequency band that the user defines. The oscilloscope employed in the time-domain measurements. Time-domain measurements permit to carry out quick measurements reducing the time spend at an EMC test laboratory.

The availability of the probability of having interference large enough to interfere is an important improvement compared with the existing standard detectors such as quasi-peak, peak or average, defined in CISPR standards, that do not give any statistical information.

Chapter 4

DC POWER QUALITY PARAMETERS AND STANDARD EMISSION LIMITS WITHIN THE RANGE 2-150kHz

An electrical power system is composed of power sources, transmission and distribution equipment and loads, which all affect the disturbance levels. All equipment is required to meet voltage and frequency distortion criteria as defined in the standards. Degradation of the performance of a power system is not only a power quality issue but also EMC related as it is affected by the interaction of the equipment. Compatibility levels are the specified electromagnetic disturbance levels used as a reference level in a specified environment for coordination in the setting of emission and immunity limits. Emission limits are the maximum emission level specified for a particular device equipment, system or disturbing installation as a whole.

As already said, for every configuration of transmission, as AC or DC, the frequency range determines different standard and power quality parameters we have to take into account. The case of disturbances emitted by DC equipment in the range 2-150kHz is one of the most discussed topics within electromagnetic compatibility of the last years. Whereas the frequency range up to 2 kHz and the frequency range starting at 150 kHz are already covered by standards, in the range 2-150 kHz (also referred to as supraharmonics) there are only few constraints due to standards for harmonic generation and a great part of power electronic converters are designed with a switching frequency within this range. Furthermore, with the increasing of the DC microgrid, HVDC transmission lines, distributed renewable energy productions, devices that work in this frequency range are increasing, too. Converters are the main disturbance generators due to their switching functioning. Very often, their switching

frequency, to improve the efficacy of the conversion and the reproduction of the requested output signals, is within the range 2-150kHz. In this frequency range the disturbances are mostly conducted, thus they propagate through cable lines to the others devices, being themselves possible disturbance generators.

For these reasons, the necessity to have standard for emission disturbances and power quality (PQ) parameters for the electric quantities within of the network comes out.

4.1 DC Power Quality Parameters

The power quality of DC network, and especially a DC smart grid where reducing of emissions, network congestions, power losses, and increasing of energy efficiency are requested, is continually subject to disturbances that might get worse. Disturbances can be generated internally of the DC micro grid, for the presence of no-linear loads, or can arrive from the external AC network, through the AC/DC converters, themselves possible generators of disturbances. If we consider a Low Voltage (LV) DC network there are many disturbances that can occur:

-Voltage fluctuations and flicker: Voltage fluctuations on Low Voltage (LV) ac networks are produced by fluctuating loads, operation of transformer tap changers (at High Voltage/Medium Voltage level) and other operational adjustments of the supply system or connected equipment. In normal circumstances voltage variation is limited to a few % of nominal voltage, but exceptional load changes or switching operations may cause voltage excursions outside normal tolerance (for example $\pm 10\%$ of nominal voltage) for hundreds of milliseconds or even tens of seconds, until onload-tap-changers on HV/MV transformers have operated. Voltage fluctuations may cause flicker. An LV dc network is connected to the LV or MV ac network, where the above described phenomena occur, through an AC/DC converter, which filters off voltage fluctuations by means of rapid dc voltage regulation.

-Voltage dip: a sudden reduction of the voltage at a point in the LV dc distribution system, followed by voltage recovery after a short period of time, from a few milliseconds up to a few seconds;

- Short interruption: the disappearance of the supply voltage at a point of the LV dc distribution system for a period of time typically not exceeding 1 minute;
- Voltage variation: a gradual change of the supply voltage to a higher or lower value than the rated voltage; the duration of the change can be short or long.
- Harmonics and interharmonics

As already said, converters and others no-linear loads are harmonic and interharmonics disturbance generators, which can worsen the DC network power quality. In AC systems, harmonic distortion is related to the fundamental component of the generic quantity Q , which is considered (either voltage or current). Thus, it is possible to define THD (Total Harmonic Distortion) [1]:

$$THD = \left[\frac{Q}{Q_1} \right]^{1/2} \quad (52)$$

where: Q_1 is the rms value of the fundamental; Q is the total rms value.

This formulation include also inter-harmonics; if they are negligible, this relationship becomes

$$THD = \left[\sum_{h=1}^H (Q_h/Q_1)^2 \right]^{1/2} \quad (53)$$

where: Q_1 is the rms value of the fundamental; Q is the total rms value; h is the harmonic order; Q_h is the rms value of harmonic component of order h . H is the upper limit.

For dc systems the term “fundamental component” has no significance and harmonic and interharmonic components are replaced by generic Low Distortion given by the total rms value of LFSD (Low Frequency Sinusoidal Disturbance) terms which is defined with respect to a DC quantity (the steady state value) instead of the fundamental component.

For LFSD distortion, the proposed [1] index D_{LFSD} is a direct translation of THD indices:

$$D_{LFSD} = \left[\sum_{k>0}^{k_{max}} (Q[k]/Q[0])^2 \right]^{1/2} \quad (54)$$

where: $Q[0]$ is the steady state dc value; $Q[k]$ is the frequency spectrum of the $q[n]$ quantity (rms); k is the frequency index between 0 and $k_{max}=F_{max}/df$; df

is the frequency resolution for the adopted time window length and time-to-frequency transform (namely, DFT). Upper frequency F_{max} is set to 2-3.6 kHz (to cover the frequency range normally set by harmonic distortion related standards) or 15/150 kHz to cover the two last subranges of EN 61000-4-16.

-The Ripple PQ index

The peak-to-peak value q_{pp} of the $q[n]$ sequence over kT samples interval (given by the ripple time window T over the sampling period $dt=1/df$, so that $kT=\text{round}(T/dt)$) is [1]:

$$q_{pp,T} = \max_{n,k} \{q[n] - q[n + k + k_T]\} \quad (55)$$

where $\max\{\}$ operation is done over admissible values of n and k , positive integers, so that the two terms between curly braces cannot be “closer” than k_T samples. The specification of the time window length T for ripple evaluation down to $6.7\mu\text{s}$ imposes a strict requirement on the minimum sampling frequency (about 1 MS/s per channel).

Considering a waveform $x(t)$ provided in the form of discrete samples $[x_i]$ for $i=1..N$, a set of statistical parameters are defined and calculated as follows [2]:

-The average DC component of $x(t)$ can be written as:

$$X_{DC} = \frac{1}{N} \sum_{i=1}^N x_i \quad (56)$$

With N being the total number of samples in each $Ta0$.

-The median of the samples defined as:

$$X_{DC,m} = x_{50\%} \quad (57)$$

-The peak-to-peak variation defined as:

$$x_{pp} = \frac{X_{max} - X_{min}}{X_{DC,m}} \quad (58)$$

Where, $X_{max} = \max_i \{x_i\}$, and $X_{min} = \min_i \{x_i\}$ $i=1 \dots N$.

-The RMS variation from the mean defined as:

$$x_E = \frac{X_E}{X_{DC}} \quad (59)$$

Where

$$X_E = \sqrt{\frac{1}{N} \sum_{i=1}^N (x_i - X_{DC})^2} \quad (60)$$

4.2 Standard Emission Limits Within the Range 2-150kHz

In figure 10, the conducted emission standard limits of a few international standard are plotted [7]. The curves represent the limits in dB μ V of the RMS value of the disturbances versus frequency. The two lower limits, the EN50065 and CISPR 15&14, are the proposed limits for broadband spurious emissions and unintentional emissions. The three higher, EN50160, EN50065general and EN50065industrial (these latest two with differences only after 100kHz), are the proposed limits for narrow-band signals as used for power-line communications.

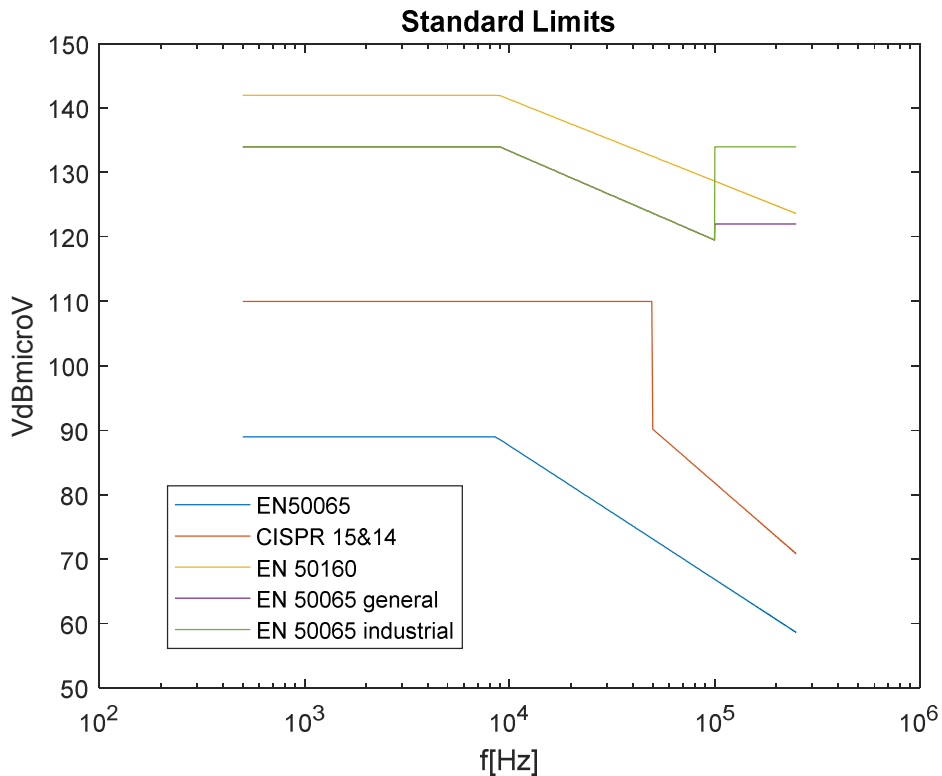


Figure 10

Chapter 5

CONVERTER CONDUCTED EMISSIONS MEASUREMENT

As already said, electronic converters are disturbance generators, especially harmonic distortion generators, so, the measurements of these disturbances is really important. In the latest years, conducted emission measurements in the frequency range 2-150kHz have become a topic more and more studied. In this frequency range the measurement have not been standardized yet, so, new studies can help to understand what might be the right for disturbance measurements.

At the University of Nottingham, United Kingdom, conducted emission disturbances, in the range 2-150kHz, of a DC/DC converters in a DC microgrid have been studied, with the usage of a LISN, remembering that the LISN is designed to measure the conducted emissions in the range 150kHz-30MHz.

5.1 Measurement Setup and its Description

The measurement setup used in the University of Nottingham Laboratory is shown in the figure 11:

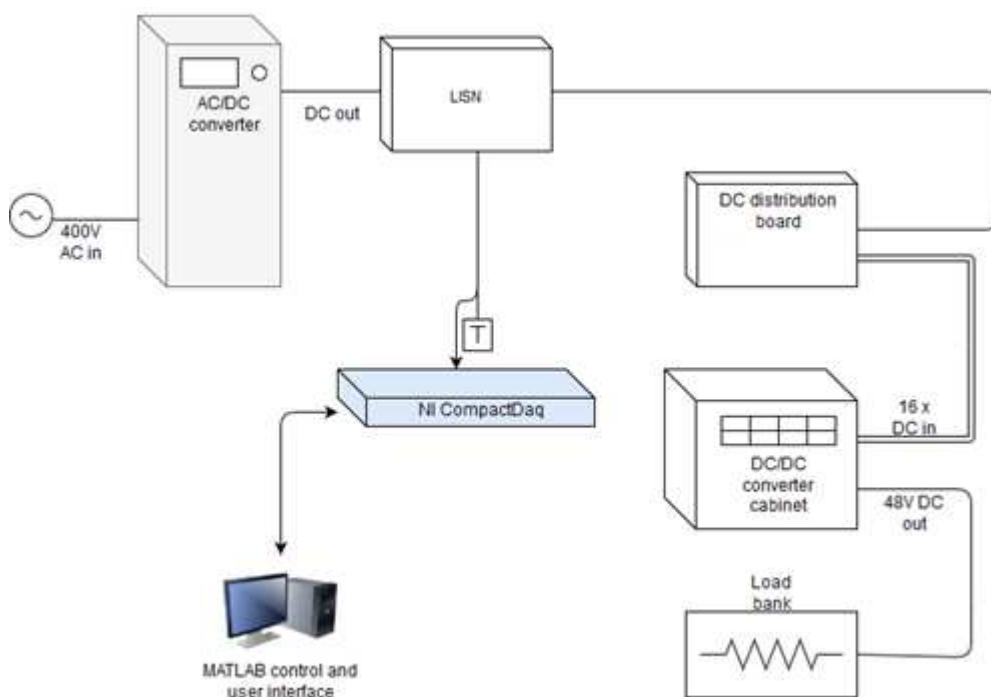


Figure 11

The circuit is composed by a AC/DC converter as the supply of the DC grid, a DC/DC Buck converter used to have always 48V at the output, which is connected to a resistive load. Between the two converters, the LISN is positioned to measure the DC/DC converter emission. The measuring port of the LISN is connected to the Laptop through an acquisition device. Then, the measured signals are elaborated with MATLAB[®].

Measurements had done changing the output voltage of the AC-DC converter (188V, 240V, 410V) while the DC-DC converter keeps its output voltage at 48V; another changing is the power requested by the load.

Devices description:

- AC/DC converter: this device is connected to the three-phase AC network. The DC output is used to vary the voltage from 188V to 410V. It has a display where it is possible to set the DC voltage and visualize the power and current absorbed by the circuit connected to the output, and other parameters as the power factor of the power absorbed from the network.
- LISN: the one used in the laboratory is a three-phase LISN, adapted to support a one-phase circuit connecting phase L1 and N. (figure 12a, 12b)

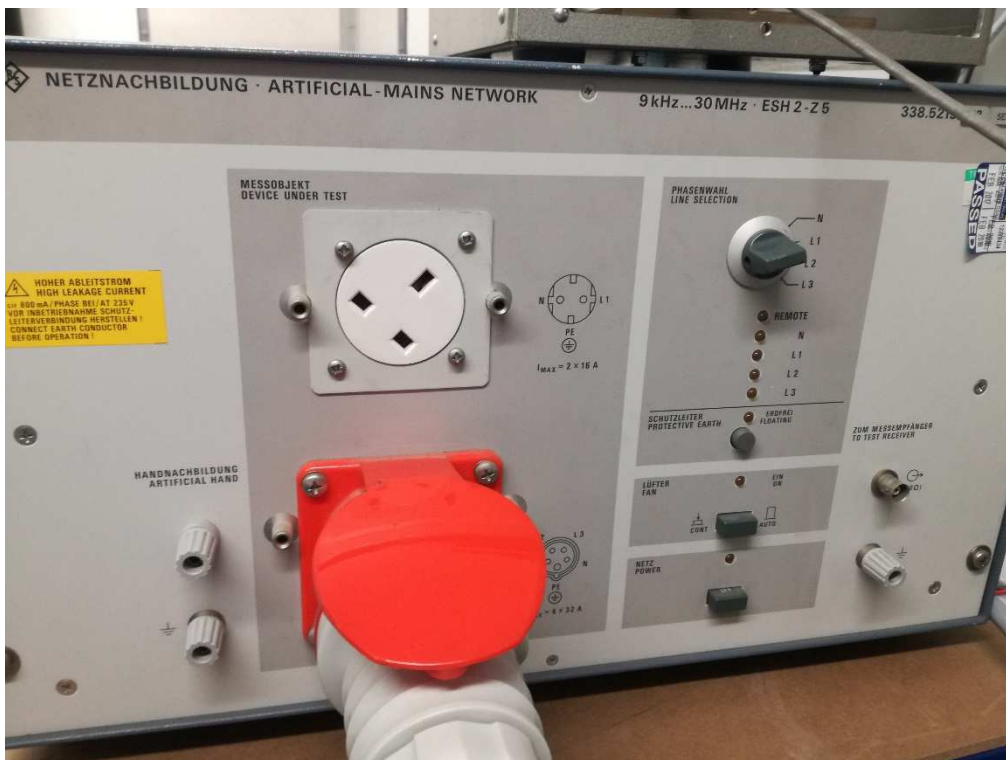


Figure 12a: front view of the LISN; it is possible to see the phase selector and the three-phase connector to the EUT (only two phase are used for this DC case).



Figure 12b: rear view of the LISN; it is possible to see the power supply connector to the AC/DC supply (only two phases are used for this DC case).

- DC/DC converter: this device is a Buck converter, with the output voltage always of 48V. It is positioned in a converter cabinet where there are more than one converter. Unfortunately, the parameters of this converter, as the switching frequency, are unknown. (Figure 13a, 13b).



Figure 13a: front view of the converters cabinet



Figure 13b: rear view of the converters cabinet

- Load Bank: it is a resistive load, of which is possible to change the value of the resistance to change the absorbed power. It is a fan load and it might be

connected to the AC network, too, absorbing powers higher than the absorbable power with a DC input of only 48V. (Figure 14a, 14b)



Figure 14a: view of the DC resistive load connectors.

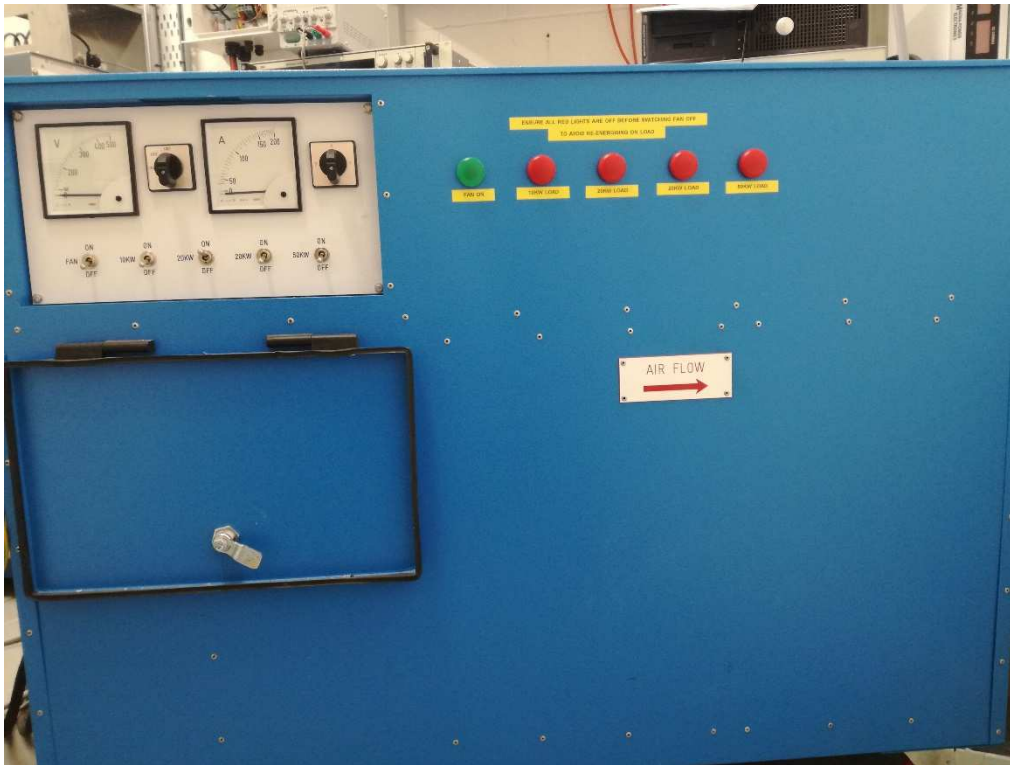


Figure 14a: front view of the DC resistive FAN load.

- Acquisition device: this National Instrument device, NI cDAQ™-9171, is used to acquire the signal measured by the LISN. It has a resolution of 32 bits. (Figure 15a, 15b).



Figure 15a, 15b

- MATLAB®: measured disturbance signals are then elaborated with the Matlab tools.

5.2 MATLAB® Scripts

Once that the devices, loads and LISN are positioned and connected together as described above, the signal measured by the LISN has to be acquired, thanks to the acquisition device, by a Matlab script function called “StartDataCpature”, written by the researcher of the Laboratory:

```
function StartDataCapture()

%Create a data acquisition session and add channels
s = daq.createSession('ni');
s.Rate = 5e+5; %Sampling frequency = 500kHz
s.DurationInSeconds = 1;

s.addAnalogInputChannel('cDAQ2Mod1',0,'Voltage'); %Channel 0 to
3

%Plot live data as it is acquired
lh = s.addlistener('DataAvailable', @PlotData);
s.NotifyWhenDataAvailableExceeds = 5e+5;

s.startBackground();

%pause(1)
%data processing

s.wait()

delete(lh)

s.release()

end

function PlotData(~,event)
    global GLOBAL_STORED_DATA;

    plot(event.TimeStamps, event.Data)

    t = event.TimeStamps;
    data = event.Data;

    data(:,1) = data(:,1);
    % data(:,2) = 10 * data(:,2);
    % data(:,3) = 100 * data(:,3);
    % data(:,4) = 0 * data(:,4);

    plot(t,data(:,1))
    legend('I')

    GLOBAL_STORED_DATA = data;
```

end

The studied frequency range is 2-150kHz so, to avoid possible error due to the Aliasing, the sampling frequency is chosen 500kHz, more than the double of 150kHz. The acquisition time is one second. The sampled signal is then stored in a vector called GLOBAL_STORED_DATA, ready to be elaborated.

First, the STFT of the signal is done, with the following script:

```
fs=500000; %sampling frequency
ts=0.2; %time of each window, 200ms
S=1/ts; %number of segment
N=fs*ts; %samples of each segment
t=1:500000; %samples of one second acquisition at 500kHz

%calculation of the STFT
Vf1=sqrt(2)/N*fft(GLOBAL_STORED_DATA(t<=100000));
Vf2=sqrt(2)/N*fft(GLOBAL_STORED_DATA(100000<t & t<=200000));
Vf3=sqrt(2)/N*fft(GLOBAL_STORED_DATA(200000<t & t<=300000));
Vf4=sqrt(2)/N*fft(GLOBAL_STORED_DATA(300000<t & t<=400000));
Vf5=sqrt(2)/N*fft(GLOBAL_STORED_DATA(400000<t & t<=500000));

Vt=zeros(N/2,1); %initialization voltage at measuring LISN port
Vot=zeros(N/2,1); %initialization absolute value of voltage at
measuring port
Votdb=zeros(N/2,1);%initialization voltage at measuring port in
db
ft=zeros(N/2,1);

for j=1:N/2
    ft(j)=(j-1)*fs/N; %frequency vector calculation
end

for j=1:N/2
    Vt(j,1)=(Vf1(j)+Vf2(j)+Vf3(j)+Vf4(j)+Vf5(j))/S; %average
voltage for each frequency
    Vot(j,1)=abs(Vt(j,1));
    Votdb(j,1)=20*log10(Vot(j,1)*1e6);
End

%LIMITS
f=500:500:250000;

Vodb1=170.5-9*log(f); %EN50065
Vodb1(f<9000)=89;

Vodb2=220-12*log(f); %CISPR 15&14
Vodb2(f<50000)=110;

Vodb3=192-5.5*log(f); %EN 50160
Vodb3(f<9000)=142;

Vodb4=188.6-6*log(f); %EN 50065 general
Vodb4(f<9000)=134;
```

```

Vodb4 (f>100000)=122;

Vodb5=188.6-6*log (f);      %EN 50065 industrial
Vodb5 (f<9000)=134;
Vodb5 (f>100000)=134;

%GRAPHS
figure
semilogx (ft, Votdb, f, Vodb3, f, Vodb2, f, Vodb1, f, Vodb4, f, Vodb5);
legend ('Votdb', 'EN50160', 'CISPR15', 'EN50065', 'EN50065general', '
EN50065industrial');
title ('Voltage Power');
xlabel ('f[Hz]');
ylabel ('VdBmicroV');

```

The sampling frequency is initialized at 500kHz, as in the acquisition script; to do the STFT of the signal, it is chosen a 200ms time window, as suggested in [9], thus, there are five calculations of the FFT, one for each of the five segments for a one second acquisition. In the calculation of the FFT, the result is multiplied by the factor $\sqrt{2}/N$ to have the Rms value of each harmonics. Then the average value of the FFT results in each 200ms window is calculated and the transformation of these results is given in dB μ V. At the end, the measured disturbances are represented, with the limits proposed, in a logarithmic scale in the frequencies axis. In this script the STFT is done without overlap and with a rectangular window.

Matlab tools have a function called “Spectrogram” that can do the STFT directly. The script may be changed as follow:

```

%calculation of the STFT
[Vf, ftspect, time]=spectrogram (GLOBAL_STORED_DATA (t<=500000), 10e
4, 0, 50000, 5e5);
c=2.62e-5; %proportional coefficient
Vf_abs=abs (Vf) *c;
[n, m]= size (Vf_abs);

Vtspect=zeros (n, 1);
Votdbspect=zeros (n, 1);

for j=1:n
    Vtspect (j, 1)=sum (Vf_abs (j, :))/m; %average voltage for each
frequency
    Votdbspect (j, 1)=20*log10 (Vtspect (j, 1) *1e6);
end

```

At first, this function was not used because the output of it had not a known correlation with the Rms value, so it was decided to calculate the STFT from the FFT of every 200ms windows. To find this proportional coefficient “c”, this test is done:

```

x=1/500000:1/500000:1;
s=sin(2*pi*2e3*x)+sin(2*pi*2.45e5*x);
[sSTFT,f,time]=spectrogram(s,10e4,0,50000,5e5);
assoluto=abs(sSTFT);
figure
spectrogram(s,5e4,0,1000,5e5)

```

The function “Spectrogram” needs, as input, the function to analyse (s), the sampling frequency (5e5=500kHz), the definition of the windows time (10e4/5e5=200ms), the overlap (0), and the frequency resolution (5e5/50000=10Hz). The output of the function is a complex value. The used input function is a sum of two sinusoidal signals at 2kHz and 245kHz, with the same amplitude of 1. Applying the STFT and the absolute value of it, and then looking where are the two components, the output values of the two components is $2.7 \cdot 10^4$. To convert this value to have the Rms value we have to multiply the “spectrogram” output for a coefficient $c=1/(\sqrt{2} \cdot 2.7 \cdot 10^4)=2.62 \cdot 10^{-5}$ equal for every frequency. It has been noticed that changing the frequency resolution, this coefficient has not to be changed (it is good to not request a frequency resolution lower than 5Hz), while changing the time wide it has to be changed.

After the time-frequency domain studies, the Amplitude Probability Distribution is calculated, to study the disturbances in a probabilistic way. To calculate the APD, this script is used:

```

[k,pts]=ecdf(abs(GLOBAL_STORED_DATA)); %cumulative probability

figure
Apd=1-k;
semilogy(pts,Apd);
title('APD');
xlabel('V[V]');

```

The APD calculation is simply done calculating the cumulative probability (k) of the absolute value of the disturbance signal measured by the LISN and doing the subtraction $APD=1-k$.

5.3 Measurement Results

The conducted emission measurements were done changing the input voltage levels of the DC/DC converter (188V, 240V, 410V) thanks to the possibility to

change the output of the AC/DC supply converter, and changing the power absorbed by the system changing the value of the FAN resistance.

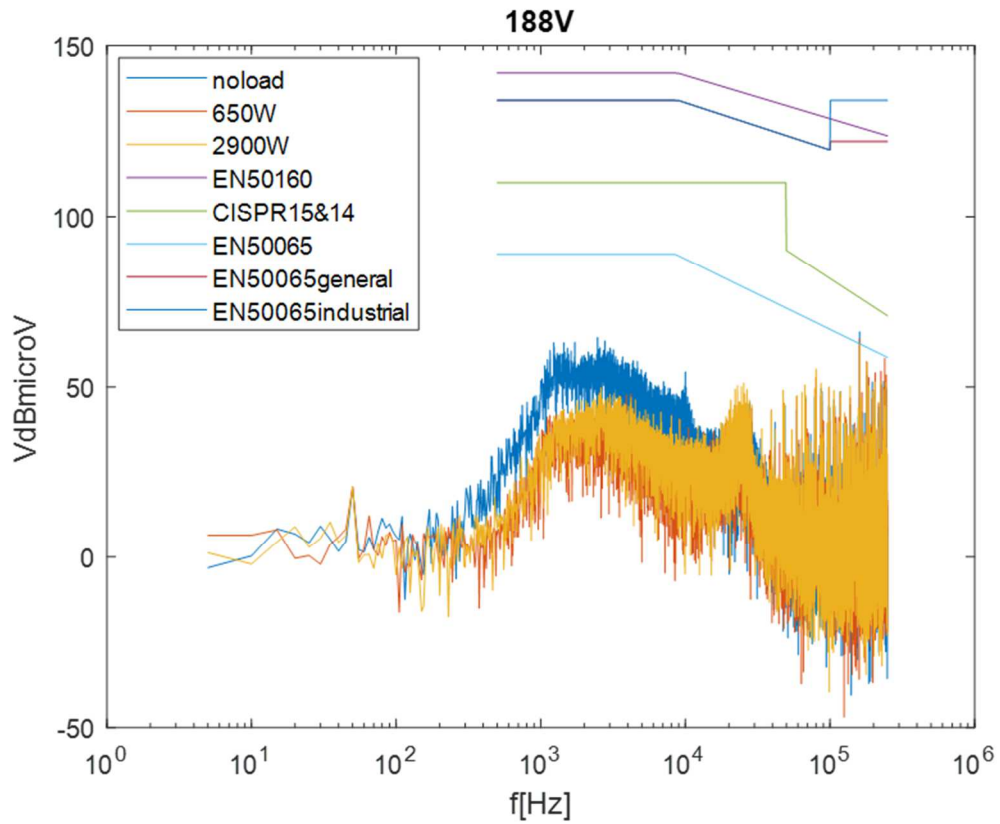


Figure 16

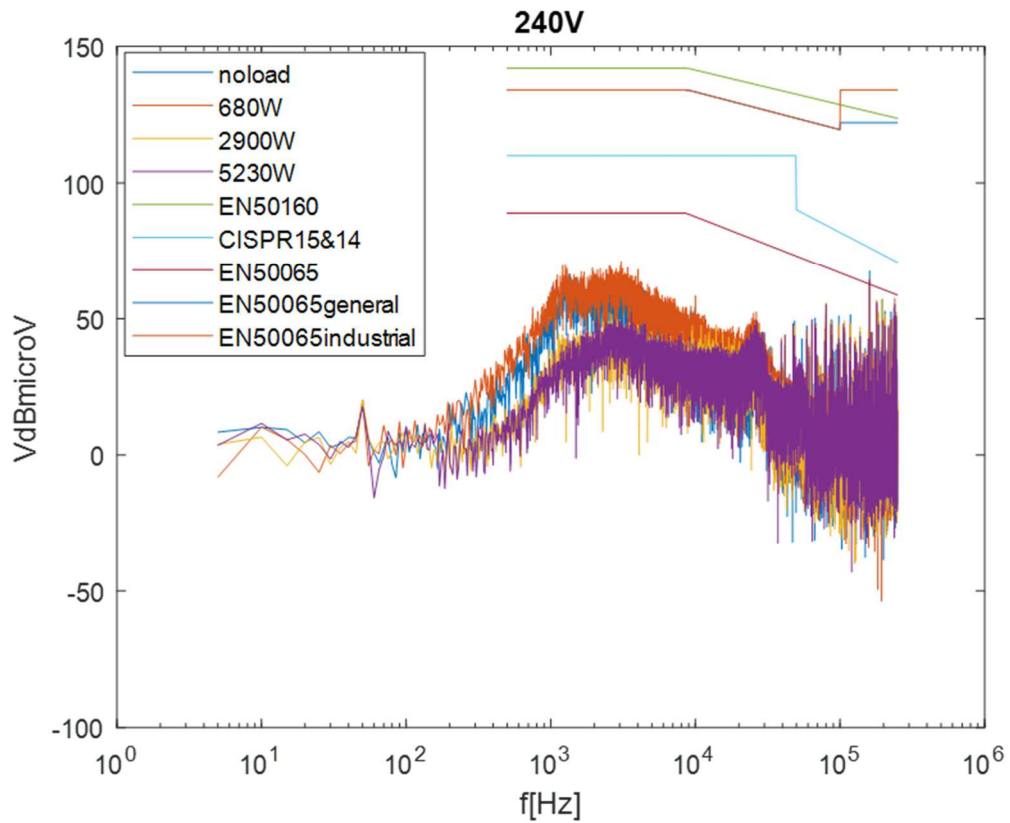


Figure 17

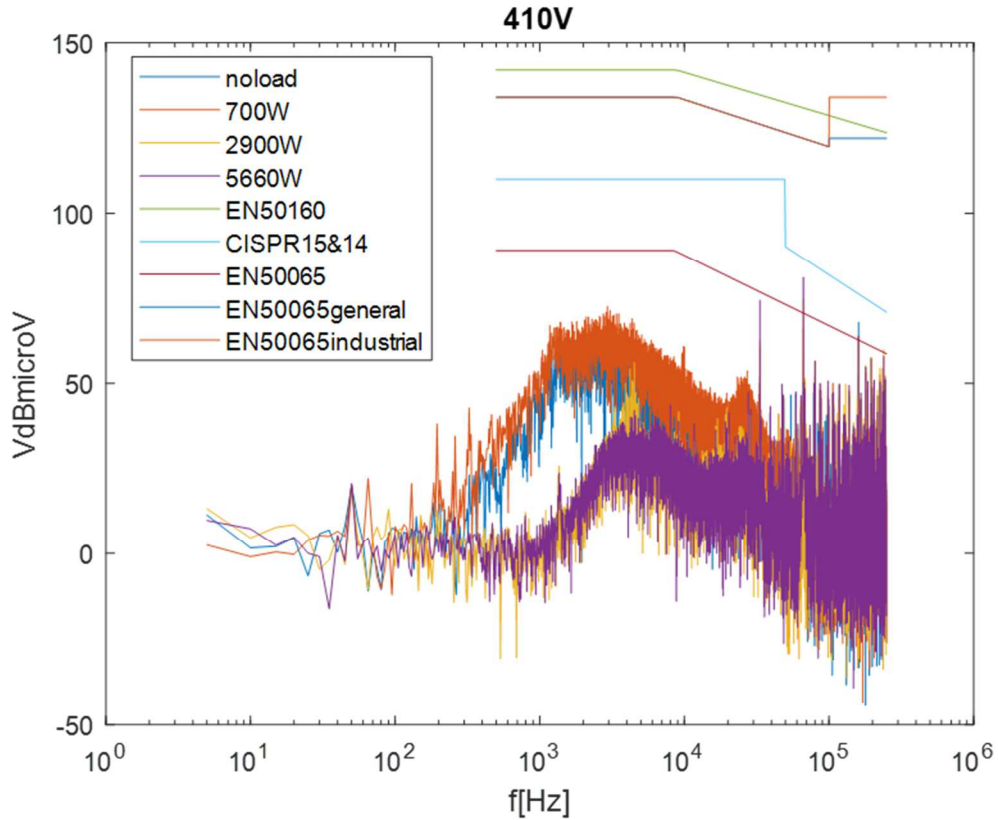


Figure 18

In figures 16, 17, 18, it is possible to see how the amplitude spectrum of the disturbances varies changing the power and the voltage. At the same voltage, it seems that for no load or very low voltage, the disturbances are higher than with higher power absorbed. At low frequencies, the disturbances are very low because the impedance of the LISN capacitor in series with the LISN signal port is too high to let pass the disturbances. Looking the curves, it seems that the switching frequency might be 20kHz (frequency used in simulation).

Table 2

<i>Vdc[V]</i>	<i>P[W]</i>	<i>P.F.</i>
188	≈0	≈0.6
188	650	1
188	2900	1
240	≈0	≈0.2-0.8
240	680	0.9
240	2900	1
240	5230	1
410	≈0	≈0.4-0.8
410	700	0.8
410	2900	1
410	5660	1

Looking at Table 2, it seems that there is a correlation between the Power Factor of the AC side and the quality of the signal. In fact, the lower the PF, the higher the disturbances.

The APD is calculated directly from the time domain measurement, even it for different power and voltage.

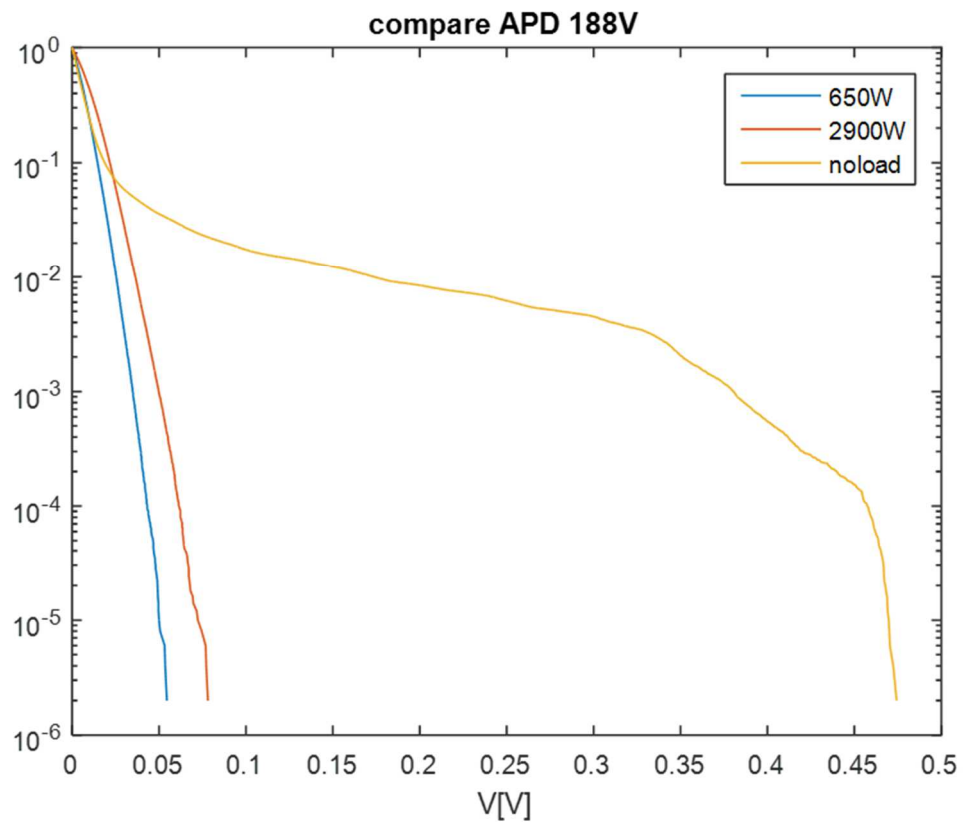


Figure 19

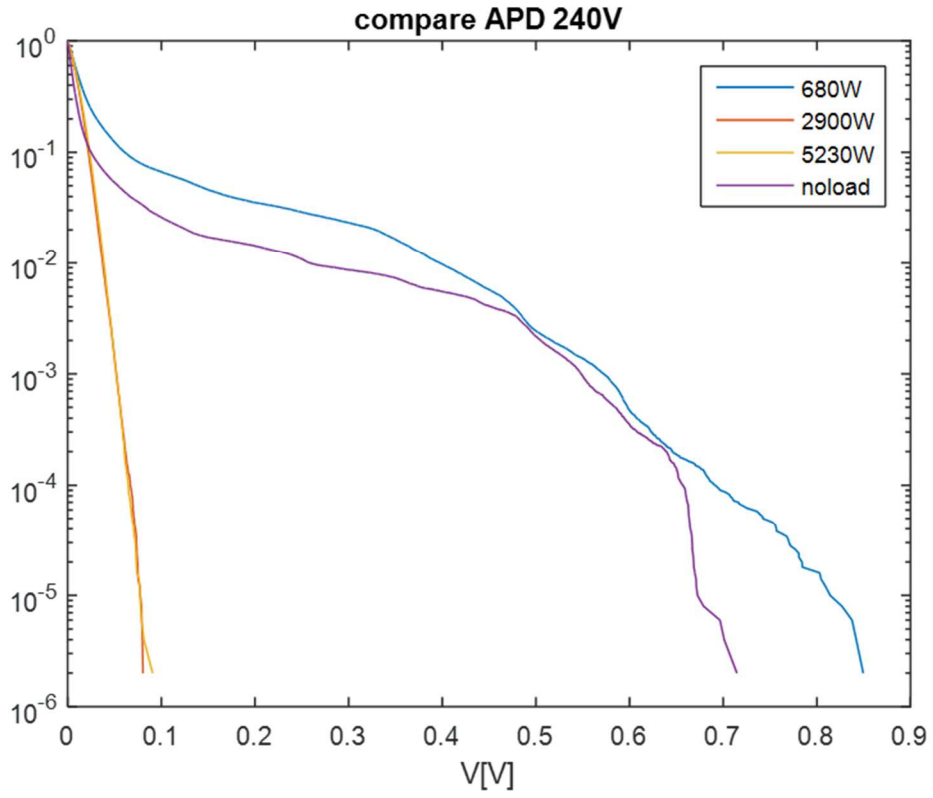


Figure 20

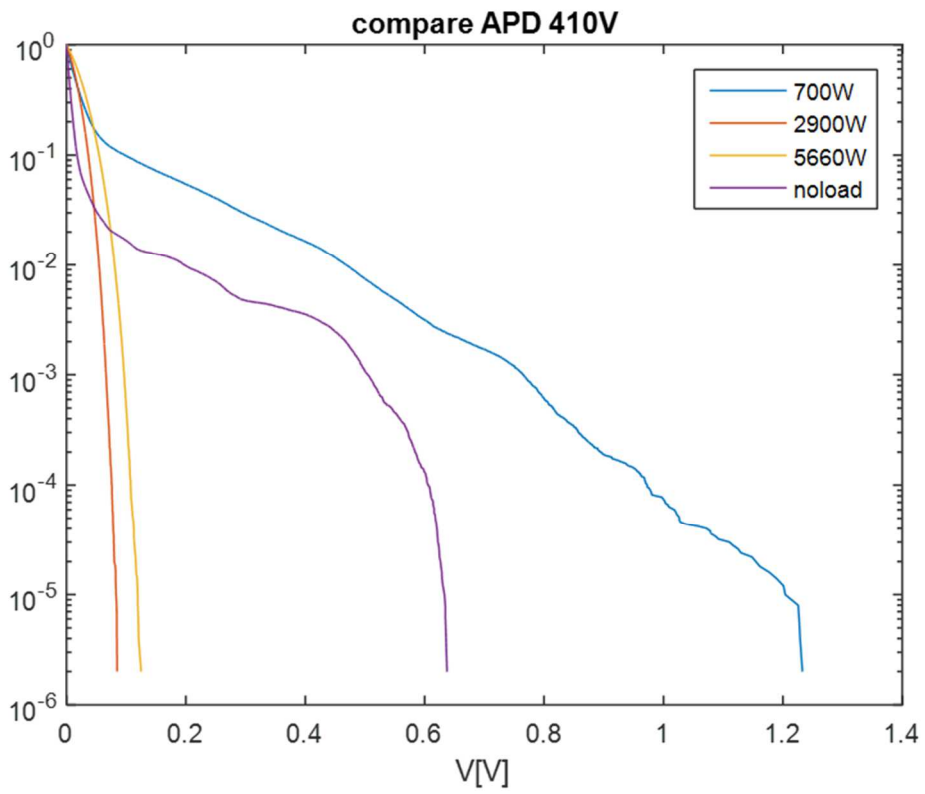


Figure 21

In the figure 16, 17, 18, it is possible to see how the probability of the disturbances varies, in function of the power requested and voltage levels. As seen for the STFT results, low power requested means higher disturbances, and here it is possible to see that for higher voltage, the disturbances can reach, with low probability, higher values ($\approx 1.2V$).

Other measurements and observations

Figure 22 is the representation in time domain and in frequency domain of converter emission measurement done in laboratory LACEM of the University of Bologna. The converter is linked to a load of about 200W, which is supplied with 385V. The measurement was done using an oscilloscope that can do the FFT with an own algorithm. The converter has a switching frequency of 100kHz that is possible to see in the graph in frequency domain.

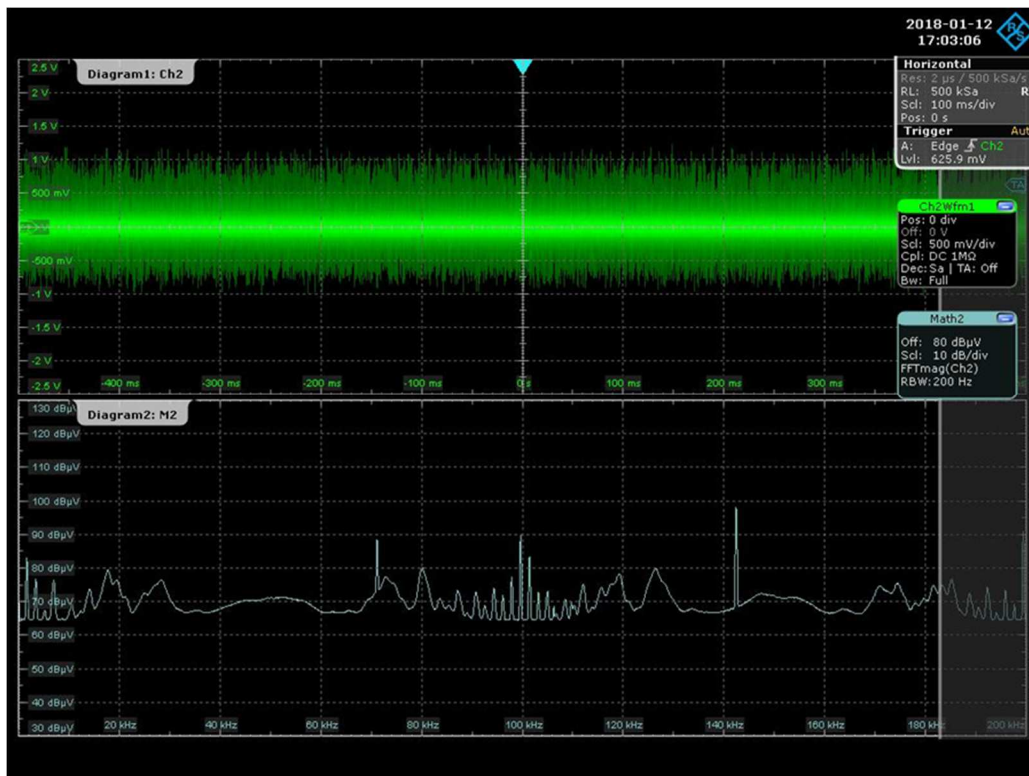


Figure 22

The time domain data have been then studied and elaborated with the Matlab script, described before.

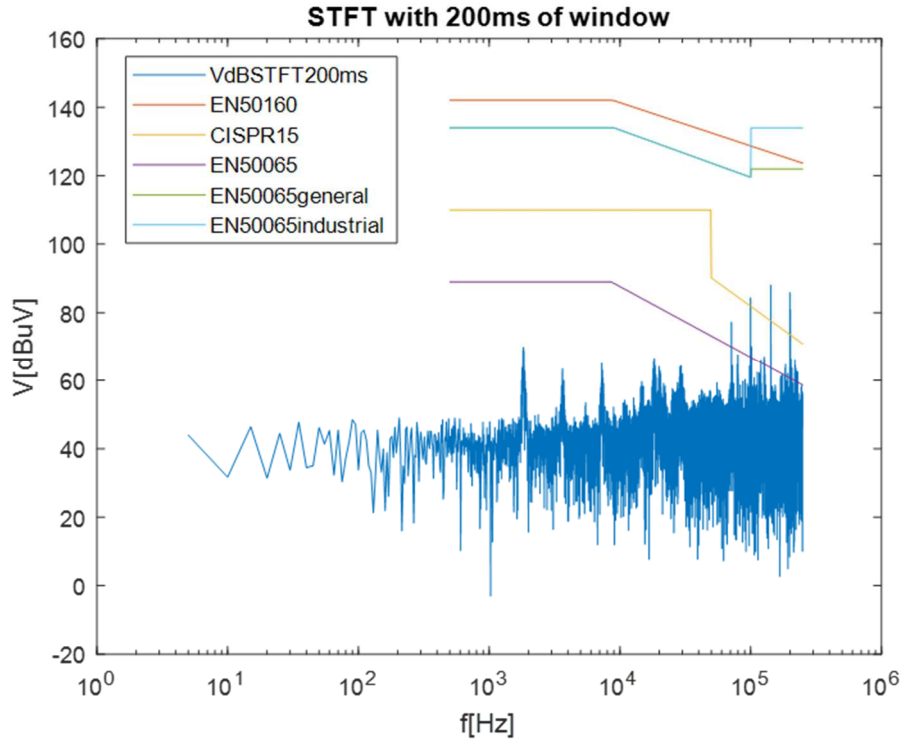


Figure 23

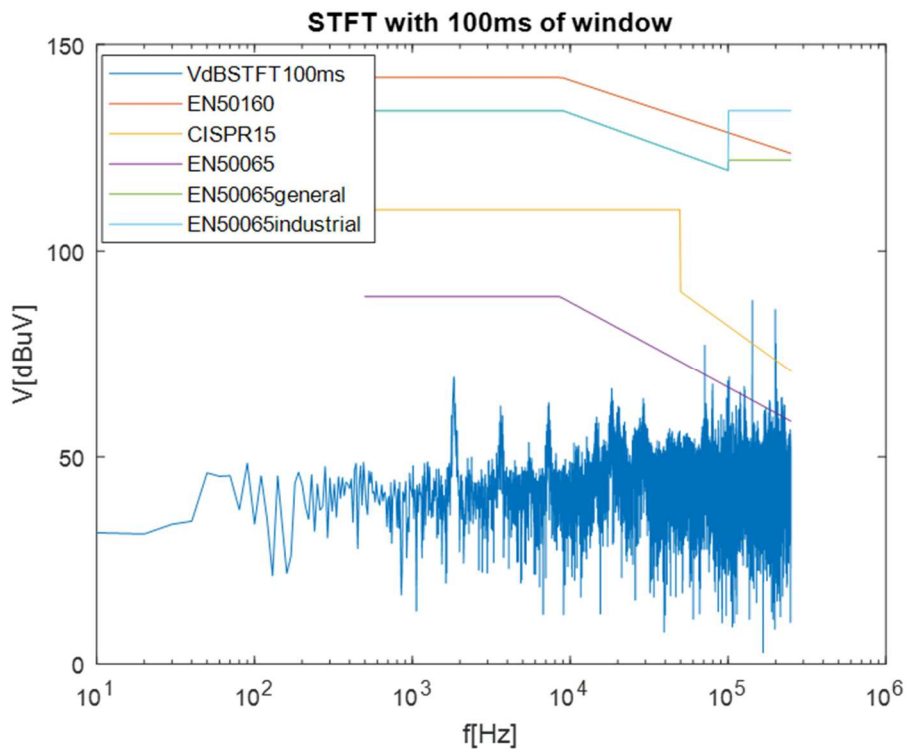


Figure 24

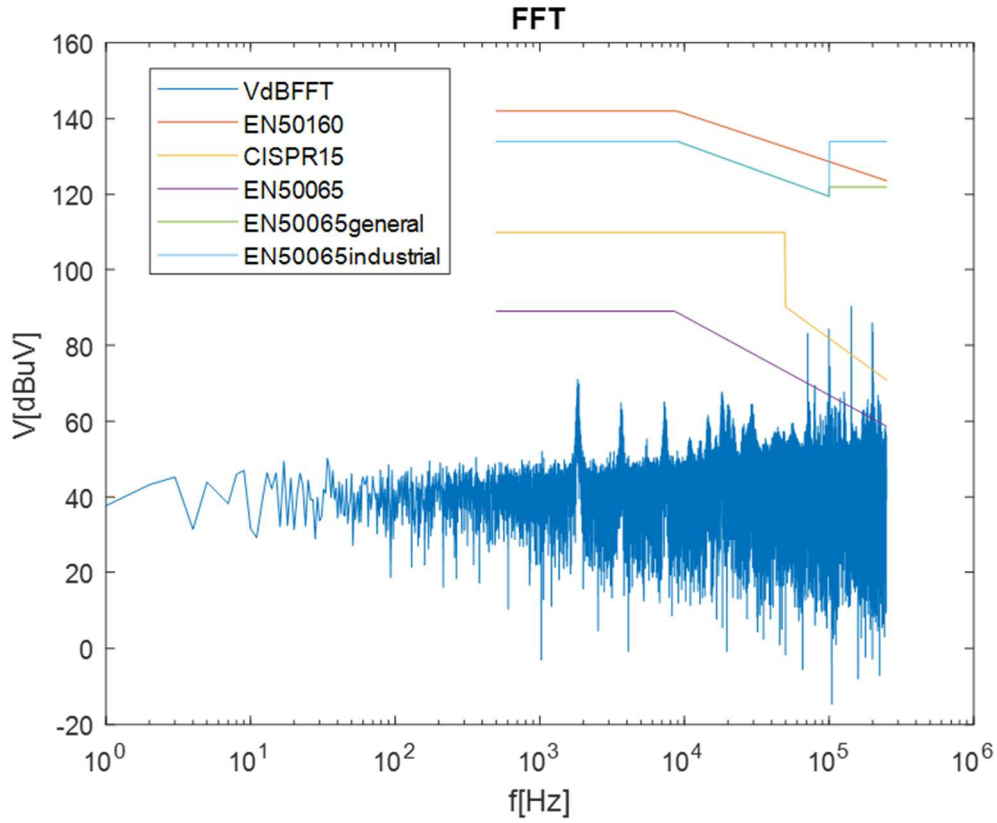


Figure 25

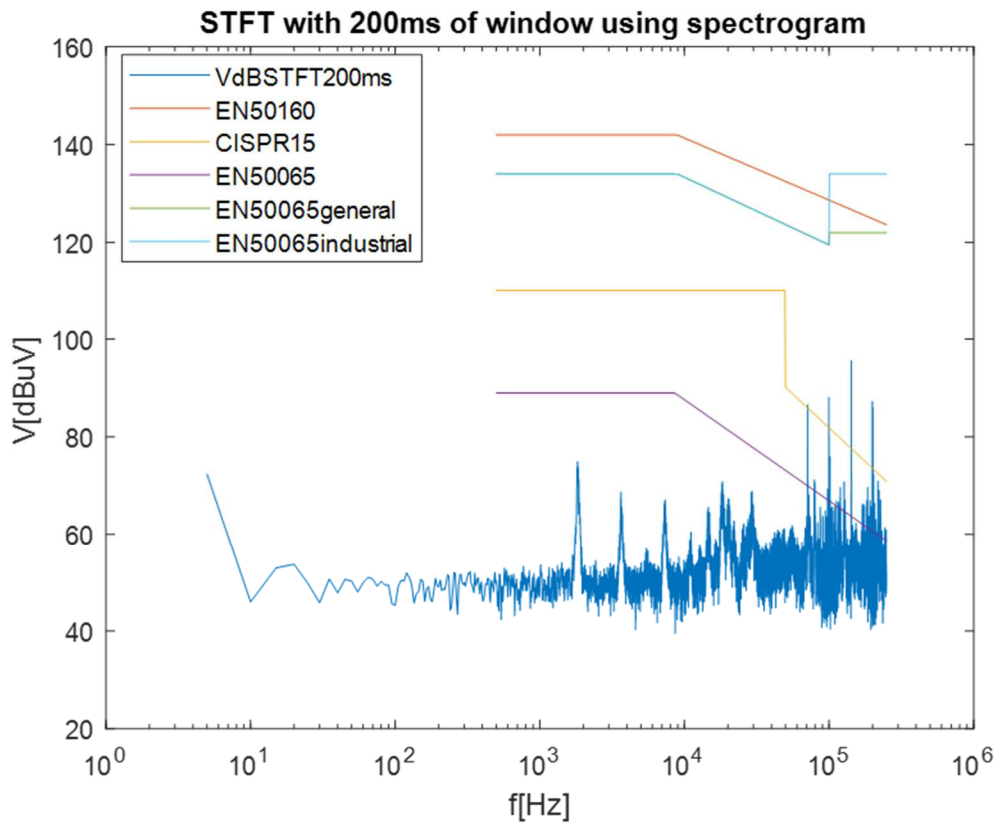


Figure 26

Figures 23 and 24 show how may be important the choice of the time width of the STFT. In fact, for the results of figure 23, a window of 200ms is used, as the normative suggest, instead, for the results of figure 24, a 100ms window is used, and it is possible to see that the peak at 100kHz, the switching frequency, is very low and not discernible.

In figure 25, the results of the FFT of the entire measured signal are shown. It shows that, studying a steady state signal and not a transient one, the FFT gives results not so different from the STFT done by the oscilloscope. Furthermore, it gives results nearer to the oscilloscope elaborating results than the STFT done using the FFT for every 200ms window (higher peak).

A further improvement is using the function “Spectrogram” directly with a frequency resolution of 5Hz: in this case, as shown in figure 26, the peak that the disturbances reach are even higher and nearer to the oscilloscope elaborating results. It was tried to use 10Hz of frequency resolution, but the results showed lower peak.

These possible errors, or at least differences, between the different ways to calculate the STFT, or simply the FFT, are curios. In fact, studying a steady state signal, the FFT and the STFT (using the FFT or the spectrogram function) calculations should give the same results.

Chapter 6

CONDUCTED EMISSIONS MEASUREMENT SIMULATION

Simulating the conducted emission might be an interesting way to know how a device may disturb an electric network. In fact, by simulation, it might be possible to see the behaviour of devices for different configuration or in different grid, before they are connected to the network, or more, before they are built, during their design.

In this specific case, conducted emission of a converter in the frequency range 2-150kHz was studied, to compare the results of the real measurements done with the LISN. The tool Simulink of Matlab[®] has been used to create a circuit that might simulate the one used for the real measurements. Then, the measurements done with the simulations have been elaborated in the same way done for the real measurement, as Fourier Transform and APD calculation.

Furthermore, in this case it was possible to change more circuit parameters and to calculate some Power Quality parameters, not calculated for the real measurement because the input voltage of the converter was not measured and acquired, and seeing how they change, changing the configuration of the simulation circuit.

6.1 Simulation Circuit

The simulation circuit used is the one shown in the figure 27, created with the Simulink-Matlab tools.

Starting from the left there are:

- Vdc: the supply DC voltage that simulates the DC output of the AC/DC converter of the laboratory.
- LISN: capacitance C_p (1 μ F), inductance L_s (50 μ H), capacitance C_1 (0.1 μ F), resistances parallel $R_m//R_1$ (\approx 50 Ω). In series of the C_p there is a resistance R_{cp} (1 Ω) because a capacitor cannot be directly connected in parallel to a voltage generator.

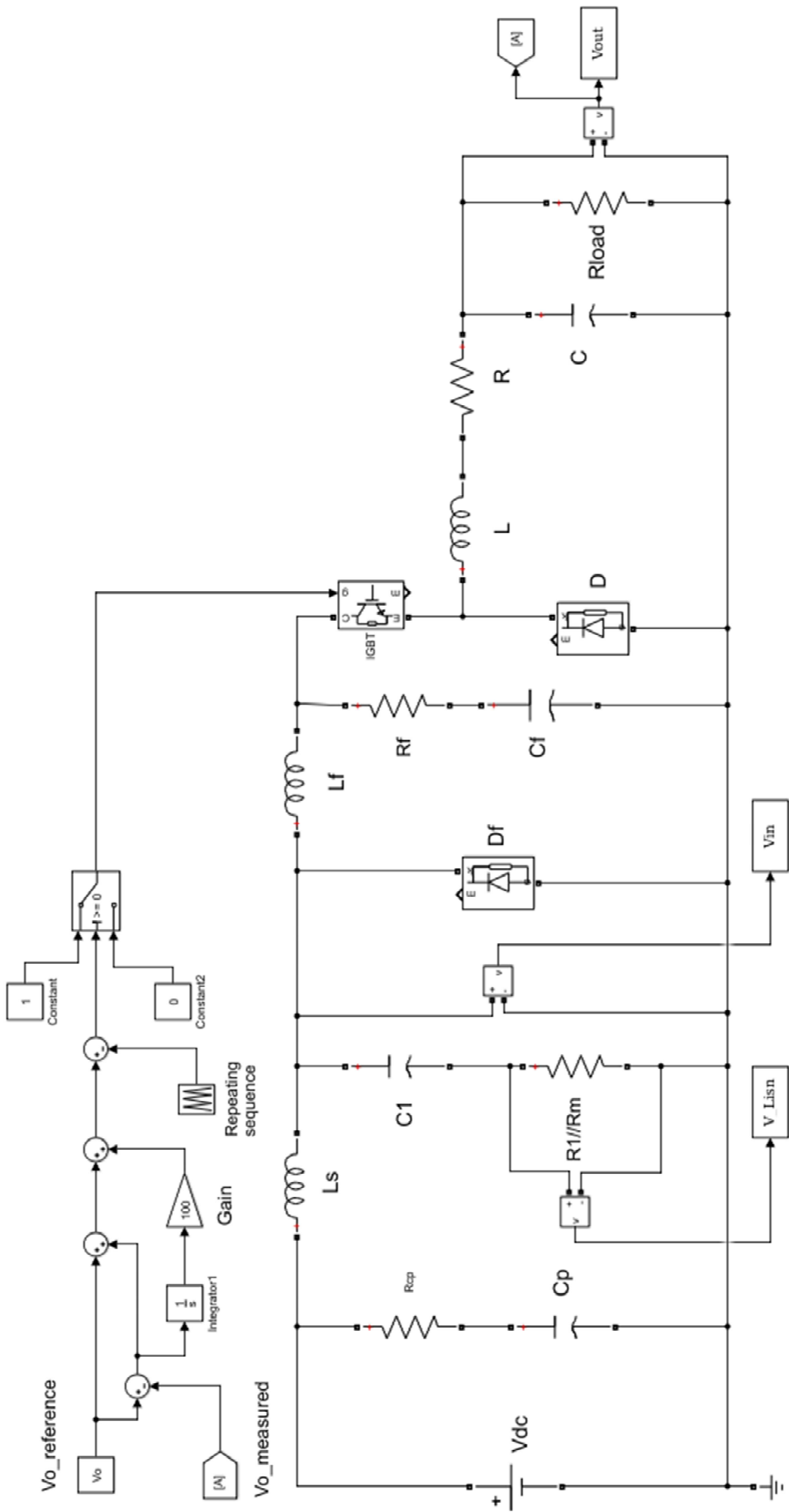


Figure 27

- Filter: diode D_f (could either be to prevent the filter from causing oscillations reaching the supply voltage on the supply or as part of a boost input stage), inductance L_f (20 μ H), resistance R_f (10m Ω), capacitance (10 μ F-variable for some simulation).
- DC/DC Buck converter: switch (IGBT), diode D , inductance L (89.7 μ H-calculated to have the converter in Continuous Mode for every supply voltage and power requested), resistance R (1m Ω), capacitance C (250 μ F-to have a low ripple of the converter output voltage at the load).
- Load: a resistance R_{load} (calculated to simulate the power requested in the real measurement: $R_{load}=V^2/P$).
- Duty cycle control: to ensure that the output voltage is the one requested (48V in this case). It makes a Proportional-Integral (PI) control, with a changeable gain (normally 100) for the Integral section, of the converter output voltage with the reference voltage, having the new reference voltage. Then it is compared with a triangular repeating sequence (with a period $T=1/f_s$, and $V_{max}=V_{dc}$; $f_s=20$ kHz to simulate the alleged switching frequency of the real converter). The output of this comparison controls the opening (signal 0) and the closing (signal 1) signal of the converter switch. It was noticed, as figure 28 shows, that removing the input filter, the duty cycle control is necessary (an impulsive signal, for the switch, related to the t_{on}/T is not enough); if there is the capacitive filter, the control is not necessary; removing the LISN, the duty cycle control is again not necessary, without the filter, too. Figure 29 shows the converter input voltage. It is possible to see that, in the presence of the LISN and without the filter, the input voltage of the converter is very variable, instead, with the filter, the input voltage has low variations from the supply voltage value, in this case 410V, and so the duty cycle control becomes unnecessary. Very probably, the LISN disturbs the input voltage due to the interaction with the switching frequency disturbances, but the capacitive filter can reduce this voltage variations.

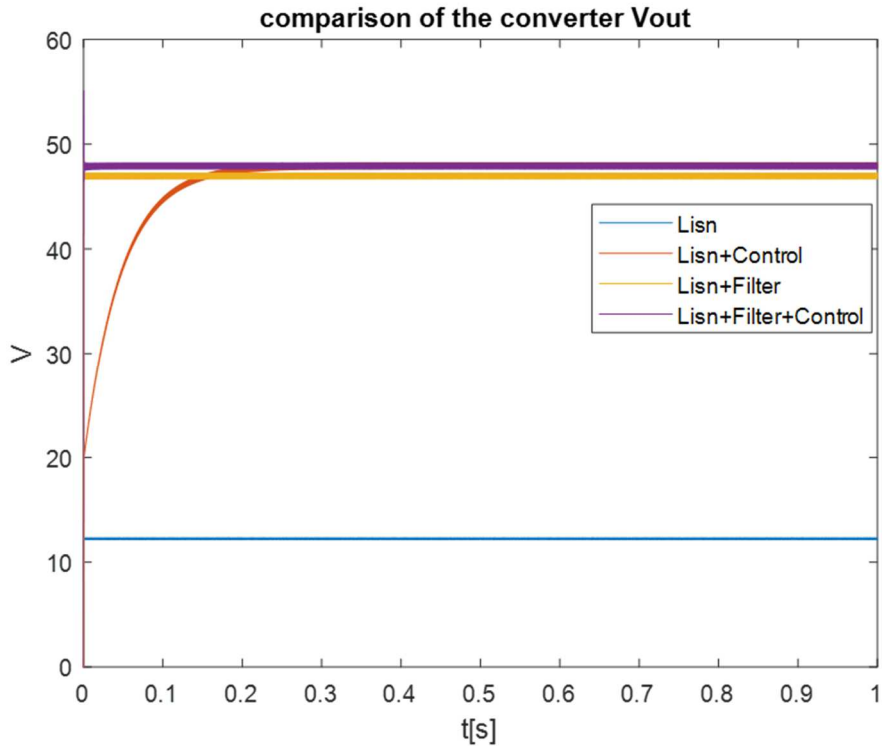


Figure 28

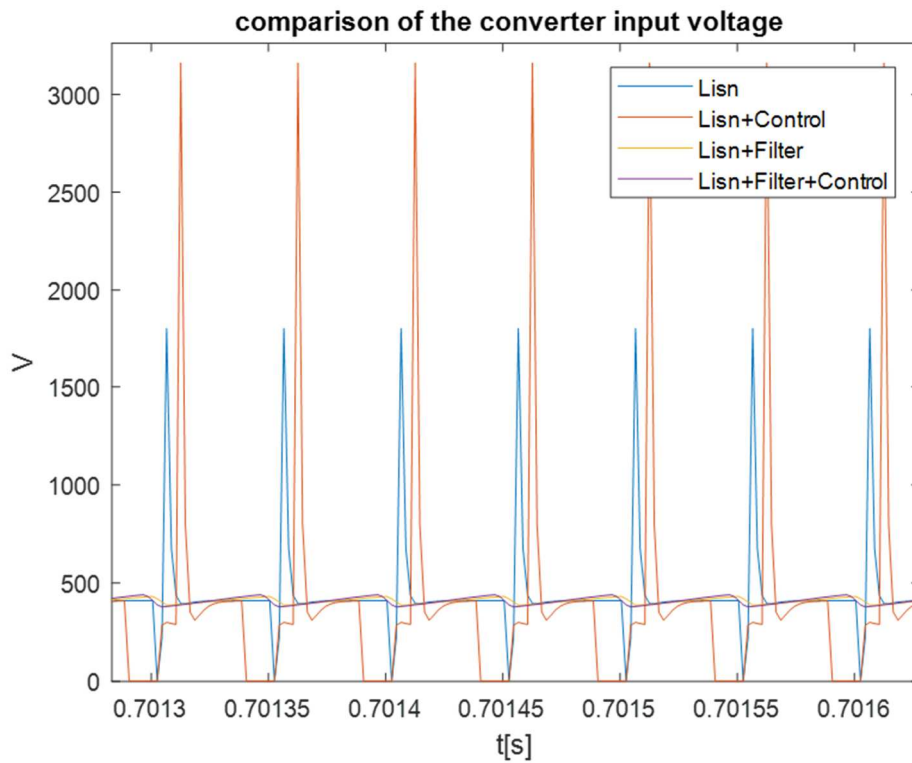


Figure 29

To elaborate the signals, the quantities measured at the simulation LISN port V_{Lisen} , at the input converter port V_{in} , and at the load V_{out} , are sent to the Workspace of Matlab.

6.2 MATLAB® Scripts

Once the circuit is drawn down, the simulation can start. The first thing to do is to run the script with the variable of the circuit, changeable from it:

```
Vdc=410; %DC voltage supply

P=700; %requested load power
Vo=48; %output voltage
R=Vo^2/P; %load resistance

d=Vo/Vdc*100; %relative duty cycle (in case the duty cycle
control is not used)
T=0.00005; %switching period
t=d*T/100; %duty cycle

L=0.6*(1-48/410)*T*(48)^2/680; %converter inductance
C=250e-6; %converter capacitance
```

The voltage supply changes to simulate the real measurement (188V, 240V, 410V); the same thing is for the power requested. The switching period, used in the control of the duty cycle, is chosen 0.0005s to have a switching frequency of 20kHz. The converter inductance is calculated to guarantee the uninterrupted current flow, to work in Continuous Mode, for every voltage levels and requested power.

After running this script and the Simulink model, elaboration of the signal is done with the following script:

```
fs=500000; %sampling frequency
ts=0.2; %time of each segment
S=1/ts; %number of segment for one second elaboration
N=fs*ts; %samples of each segment
t=1:1000000; %samples for two seconds simulation

Vdc=410;

%FFT
N2=length(V_Lisn(t>500000));
V_LisnF=sqrt(2)/N2*fft(V_Lisn(t>500000));
figure
plot(abs(V_LisnF));
legend('VLisnF');
title('FFT');
xlabel('f[Hz]');
ylabel('V[V]');

%STFT of V_LISN with 200ms windows
V_LisnF1=sqrt(2)/N*fft(V_Lisn(t<=100000));
V_LisnF2=sqrt(2)/N*fft(V_Lisn(100000<t & t<=200000));
V_LisnF3=sqrt(2)/N*fft(V_Lisn(200000<t & t<=300000));
V_LisnF4=sqrt(2)/N*fft(V_Lisn(300000<t & t<=400000));
V_LisnF5=sqrt(2)/N*fft(V_Lisn(400000<t & t<=500000));
V_LisnF6=sqrt(2)/N*fft(V_Lisn(500000<t & t<=600000));
```

```

V_LisnF7=sqrt(2)/N*fft(V_Lisn(600000<t & t<=700000));
V_LisnF8=sqrt(2)/N*fft(V_Lisn(700000<t & t<=800000));
V_LisnF9=sqrt(2)/N*fft(V_Lisn(800000<t & t<=900000));
V_LisnF10=sqrt(2)/N*fft(V_Lisn(900000<t & t<=1000000));

V_LisnF=zeros(N/2,1);
V_LisndB=zeros(N/2,1);
for j=1:N/2
V_LisnF(j,1)=(V_LisnF6(j)+V_LisnF7(j)+V_LisnF8(j)+V_LisnF9(j)+
V_LisnF10(j))/S;
V_LisndB(j,1)=20*log10(abs(V_LisnF(j,1))*1e6);
end

ft=zeros(N/2,1);
for j=1:N/2
ft(j)=(j-1)*fs/N;
end

%STFT of Vin with 200ms windows
Vin=Vin;
VinF1=sqrt(2)/N*fft(Vin( t<=100000));
VinF2=sqrt(2)/N*fft(Vin(100000<t & t<=200000));
VinF3=sqrt(2)/N*fft(Vin(200000<t & t<=300000));
VinF4=sqrt(2)/N*fft(Vin(300000<t & t<=400000));
VinF5=sqrt(2)/N*fft(Vin(400000<t & t<=500000));
VinF6=sqrt(2)/N*fft(Vin(500000<t & t<=600000));
VinF7=sqrt(2)/N*fft(Vin(600000<t & t<=700000));
VinF8=sqrt(2)/N*fft(Vin(700000<t & t<=800000));
VinF9=sqrt(2)/N*fft(Vin(800000<t & t<=900000));
VinF10=sqrt(2)/N*fft(Vin(900000<t & t<=1000000));

VinF=zeros(N/2,1);
VindBCf=zeros(N/2,1);
for j=1:N/2
VinF(j,1)=(VinF6(j)+VinF7(j)+VinF8(j)+VinF9(j)+VinF10(j))/S;
VindBCf(j,1)=20*log10(abs(VinF(j,1))*1e6);
end

%Power Quality Parameters

O=zeros(29999,1);
for j=2:30000 %f=150kHz is the 30000 sample of Vin
O(j,1)=(abs(VinF(j,1))/Vdc)^2;
end
LFSD_150kHzinVdc=sqrt(sum(O(:,1)))*100 %Low Frequency Sinusoidal
Disturbance until 150kHz

Q=zeros(1799,1);
for j=2:1800 %f=9kHz is the 1800 sample of Vin
Q(j,1)=(abs(VinF(j,1))/Vdc)^2;
end
LFSD_9kHzinVdc=sqrt(sum(Q(:,1)))*100 %Low Frequency Sinusoidal
Disturbance until 9kHz

N1=fs*2; %samples for two seconds simulation
Xdc=1/(N1-500000)*sum(Vin(500000<t))%average Vin DC component
XEIn=sqrt(1/(N1-500000)*sum((Vin(500000<t)-Xdc).^2));
xEIn=XEIn/Xdc %RMS variation from the mean

%LIMITS

```

```

f=500:500:250000;

Vodb1=170.5-9*log(f); %EN50065
Vodb1(f<9000)=89;

Vodb2=220-12*log(f); %CISPR 15&14
Vodb2(f<50000)=110;

Vodb3=192-5.5*log(f); %EN 50160
Vodb3(f<9000)=142;

Vodb4=188.6-6*log(f); %EN 50065 general
Vodb4(f<9000)=134;
Vodb4(f>100000)=122;

Vodb5=188.6-6*log(f); %EN 50065 industrial
Vodb5(f<9000)=134;
Vodb5(f>100000)=134;

%GRAPHS
figure
semilogx(ft,V_LisndB,f,Vodb3,f,Vodb2,f,Vodb1,f,Vodb4,f,Vodb5);
legend('VLisn','EN50160','CISPR15&14','EN50065','EN50065general',
'EN50065industrial');
title('');
xlabel('f[Hz]');
ylabel('VdBmicroV');

%APD
[k,pts]=ecdf(abs(V_Lisn)); %cumulative probability

figure
Apd=1-k;
semilogy(pts,Apd);
title('APD');
xlabel('V[V]');

```

In this script the FFT of the simulated voltage measured at the LISN is first done. Then, the STFT of the same voltage is done applying the FFT to every 200ms time window, without the use of any windowing (rectangular windowing by default). Due to the initial simulation transients, the simulation time was set to 2 seconds and, to avoid the transients, the last second is the one elaborated. STFT was applied to the simulated voltage measured at the converter input. Doing that, the calculation of some Power Quality parameters was possible: the Low Frequency Sinusoidal Disturbance (calculated up to 9kHz and up to 150kHz), the average DC component, the Rms variation from the mean. Then the simulated voltage measured at the LISN, already transformed in dB μ V, was plotted in a graph with the proposed standard limits. Finally, the APD of the simulated voltage measured at the LISN was calculated in the same way of the real measurements.

6.3 Simulation Results

With the aim to see if a Simulink simulation could represent the real converter behaviour some different simulations have been done.

Figures 30, 33, 36 represent quantities in time domain, while 31, 32, 34, 35, 37 represent quantities in frequency domain (obtained with STFT that gives time-domain results, but being in steady state is possible to consider only the frequency domain).

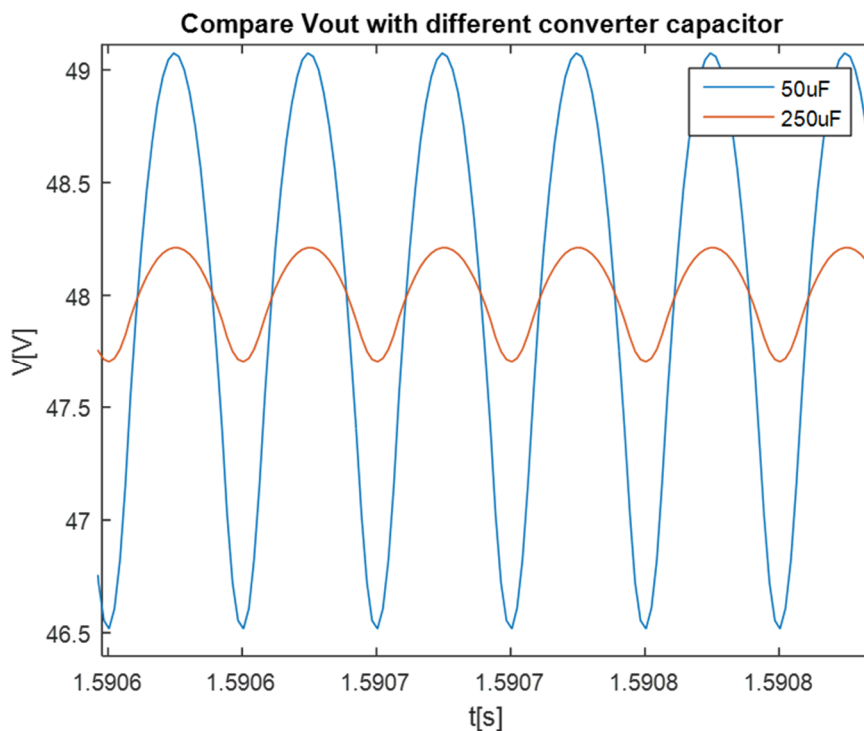


Figure 30-comparison of the output voltage of the converter using different converter capacitance. The simulation is done with a V_{dc} of 188V and a power requested of 680W. With a capacitance of 50µF, the ripple is maybe too high, thus, for the other simulations, the 250µF capacitance is chosen.

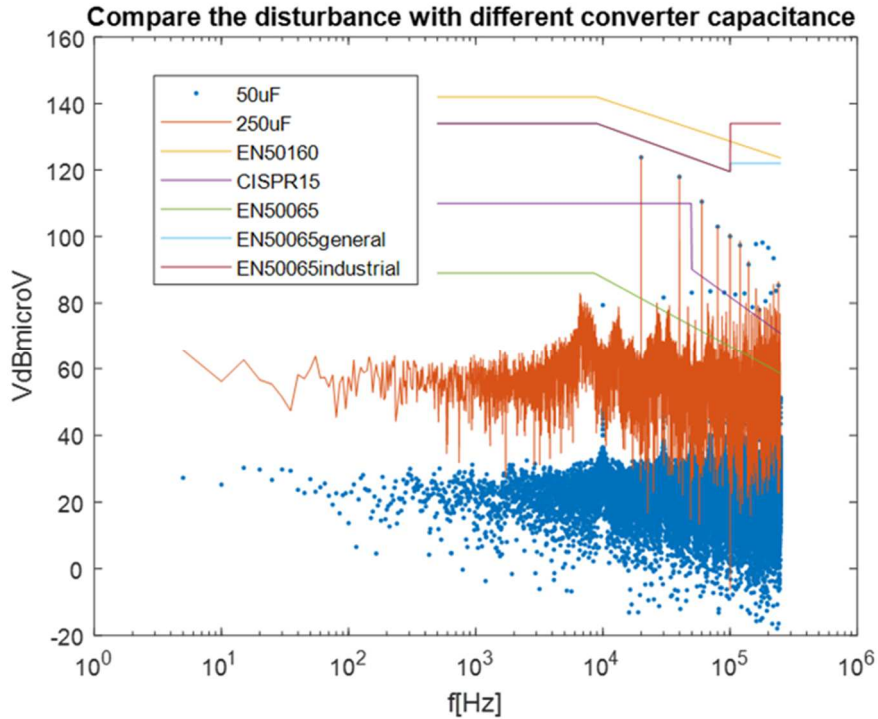


Figure 31-comparison of the voltage measured at the LISN using different converter capacitance. It shows that with a higher converter capacitance the disturbance are higher, thus, the choice of this element may be a compromise between output ripple and conducted emissions.

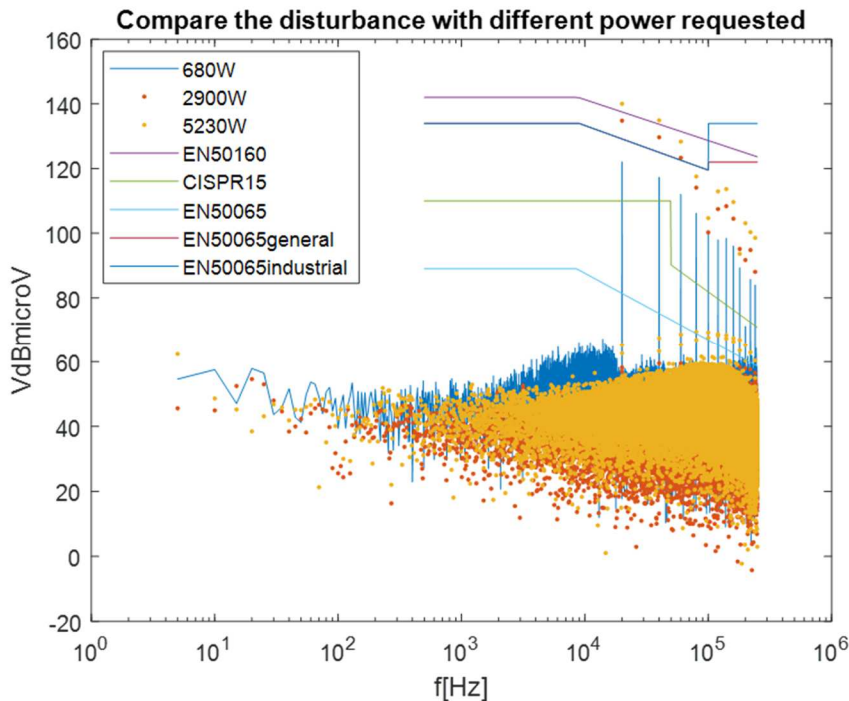


Figure 32-comparison of the voltage measured at the LISN with different requested power. It is done with a $V_{dc}=240V$. It shows that the disturbances are a bit higher for low power for frequencies lower than the switching

frequency (20kHz), then, especially the peaks obtained for this frequency and its multiples, are higher for higher power.

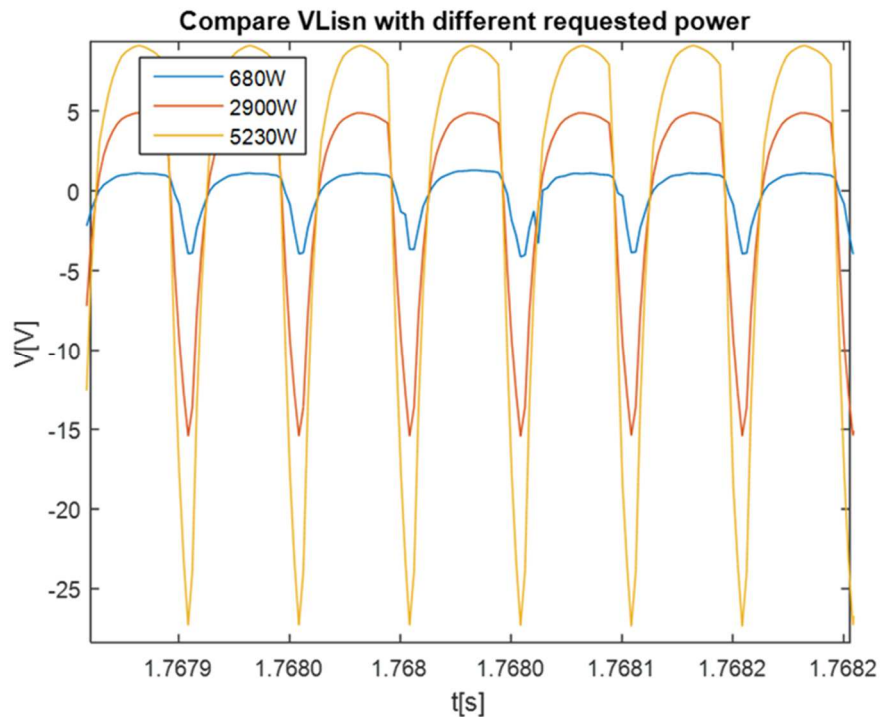


Figure 33-comparison of the voltage measured at the LISN with different requested power in time domain. The simulation configuration is the same of the previous figure, in fact, as the peaks were higher for higher power at the switching frequency and its multiples, here the disturbances reach higher value, especially negatives, for high power.

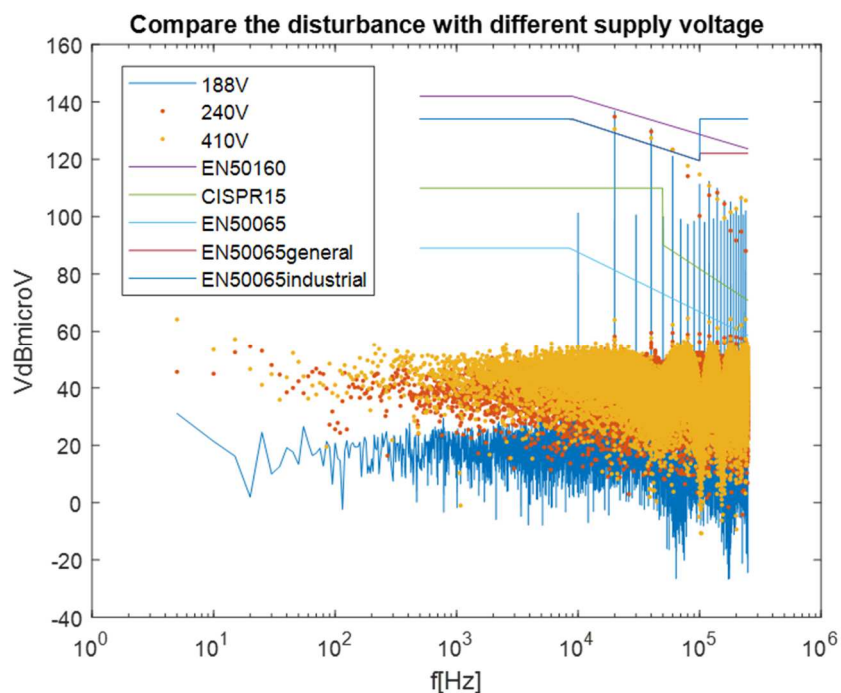


Figure 34-comparison of the voltage measured at the LISN with different supply voltage Vdc. It is done with a requested power of 2900W. It is possible to see that, normally, with the lowest voltage (188V-blue line) the disturbances are lower, but not at the switching frequency and its multiples.

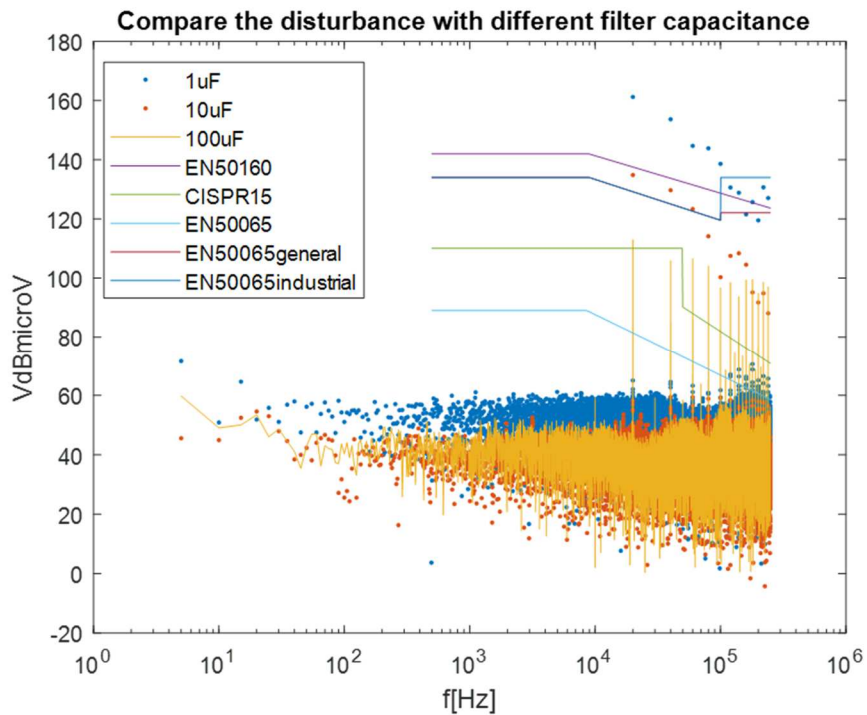


Figure 35-comparison of the voltage measured at the LISN using different filter capacitance. It is done with a requested power of 2900W and a Vdc=240V. It is possible to see that, obviously, the lower is the filter capacitance, the higher are the disturbances, especially at the switching frequency and its multiples.

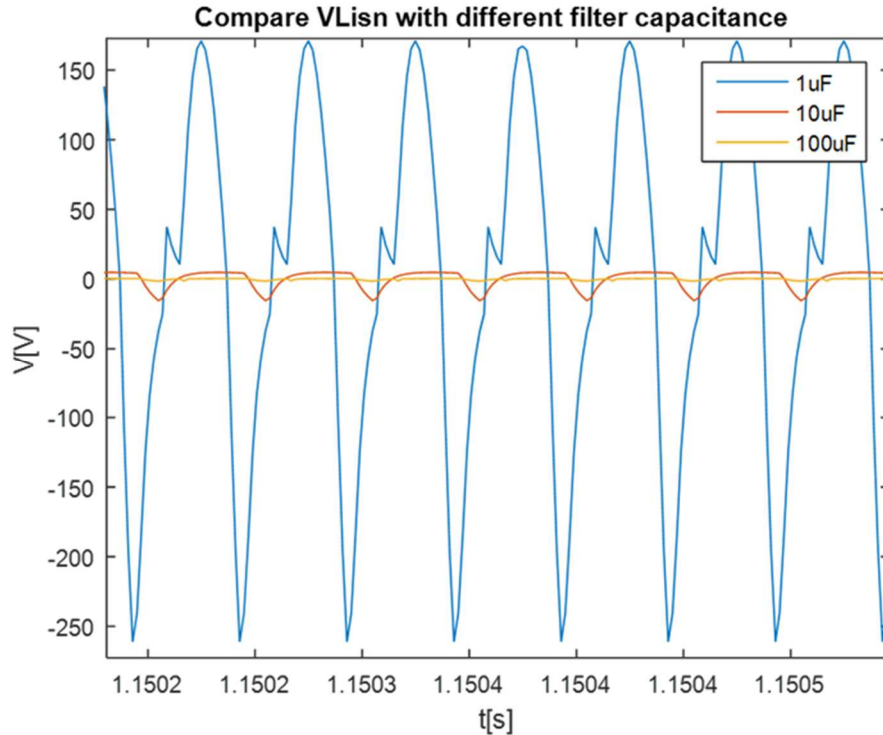


Figure 36-comparison of the voltage measured at the LISN using different filter capacitance in time domain. As already said, lower is the filter capacitance, higher are the disturbances.

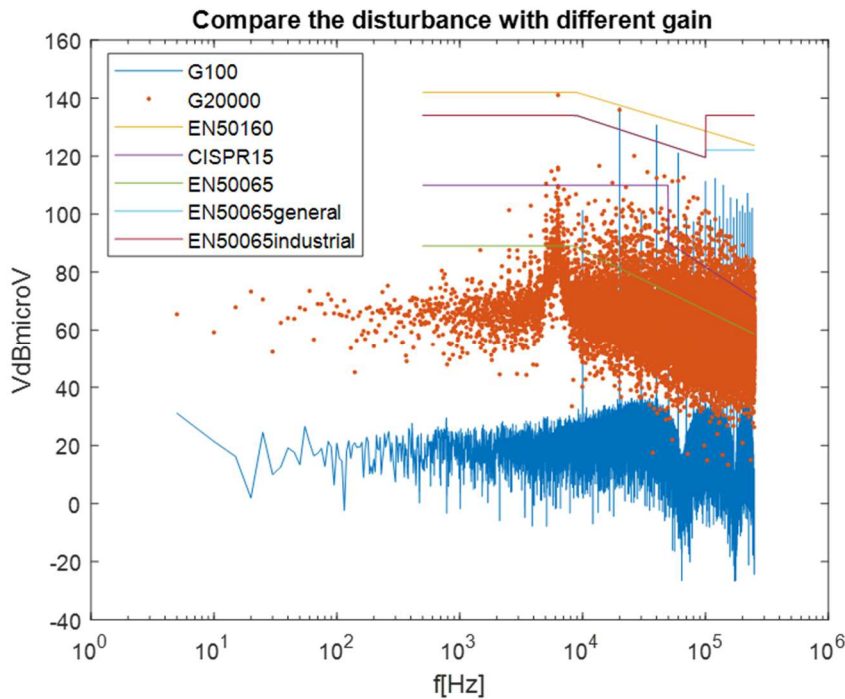


Figure 37-comparison of the voltage measured at the LISN using different gain for the duty cycle's feedback control. It is done with a requested power of 2900W and $V_{dc}=240V$. It is possible to see that if the gain is too high, the

disturbances are very high, not only at the switching frequency. It was seen that a too high gain may generate instability in the output voltage.

Low Frequency Sinusoidal Disturbance and RMS variation from the mean (x_E)

Table 3

<i>Data</i>	<i>LFSD_9kHz</i>	<i>LFSD_150kHz</i>	<i>x_E</i>
<i>Vdc=188V(P=2900W)</i>	<i>2.55*10⁻⁴</i>	<i>7.13</i>	<i>0.071</i>
<i>Vdc=240V(P=2900W)</i>	<i>0.002</i>	<i>4.67</i>	<i>0.047</i>
<i>Vdc=410V(P=2900W)</i>	<i>0.002</i>	<i>1.74</i>	<i>0.017</i>
<i>C=50uF(P=680W)</i>	<i>3.26*10⁻⁴</i>	<i>1.74</i>	<i>0.017</i>
<i>C=250uF(P=680W)</i>	<i>0.050</i>	<i>1.75</i>	<i>0.018</i>
<i>G=100(P=2900W)</i>	<i>2.55*10⁻⁴</i>	<i>7.13</i>	<i>0.071</i>
<i>G=20 000(P=2900W)</i>	<i>31.02</i>	<i>31.69</i>	<i>0.400</i>
<i>P=680W(Vdc=240V)</i>	<i>0.008</i>	<i>1.15</i>	<i>0.016</i>
<i>P=2900(Vdc=240V)</i>	<i>0.002</i>	<i>4.67</i>	<i>0.047</i>
<i>P=5230W(Vdc=240V)</i>	<i>0.003</i>	<i>8.39</i>	<i>0.084</i>
<i>Cf=1uF(2900W,240V)</i>	<i>0.013</i>	<i>94.66</i>	<i>0.950</i>
<i>Cf=10uF(2900W,240V)</i>	<i>0.002</i>	<i>4.67</i>	<i>0.047</i>
<i>Cf=100uF(2900W,240V)</i>	<i>0.003</i>	<i>0.46</i>	<i>0.047</i>

Table 3 shows how the Power Quality parameters change with different simulation conditions. They are calculated, as already said in the script description, from the voltage measured at the input of the converter, so they represent the quality of the input voltage at the converter, thus of the grid connected to it. It is possible to see that they vary as the disturbances, previously represented, varied. LFSD calculation has, at the denominator, the DC voltage; this is the reason why it is lower for higher supply voltage, in the case up to 150kHz, though the disturbances shown in the figure 34 are similar or even higher for higher voltage.

The APD is calculated directly from the time domain measurement at the LISN with the same changes used for the previous representations.

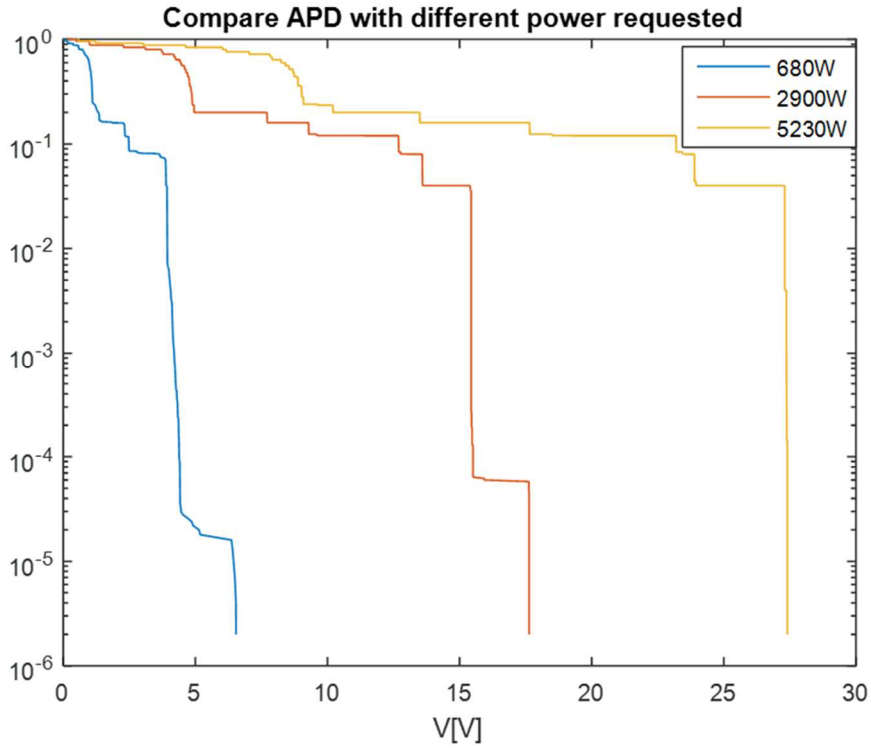


Figure 38-comparison the APD of the voltage measured at the LISN with different requested power

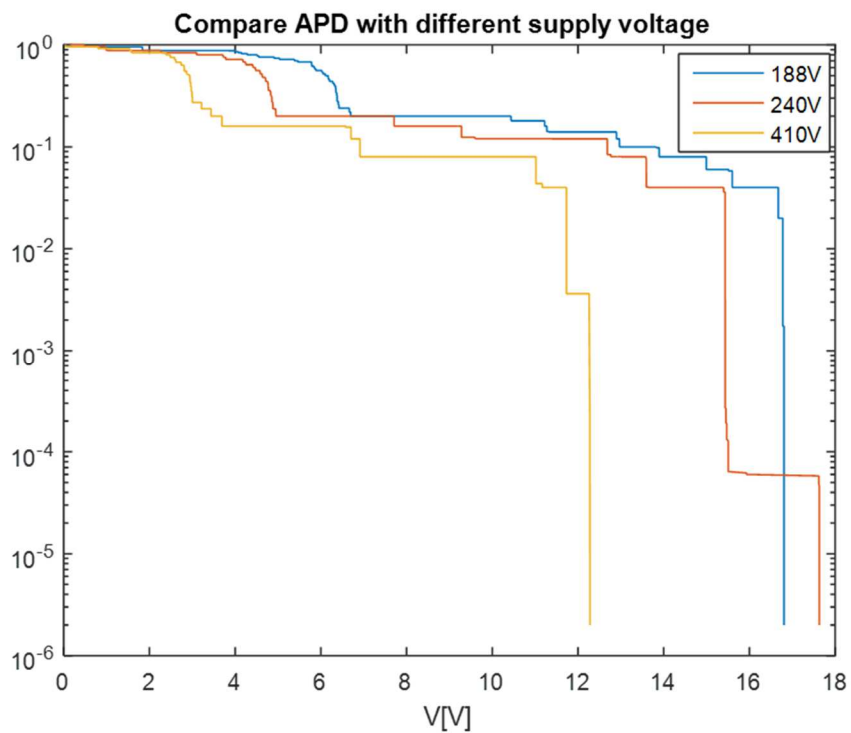


Figure 39-comparison the APD of the voltage measured at the LISN with different supply voltage.

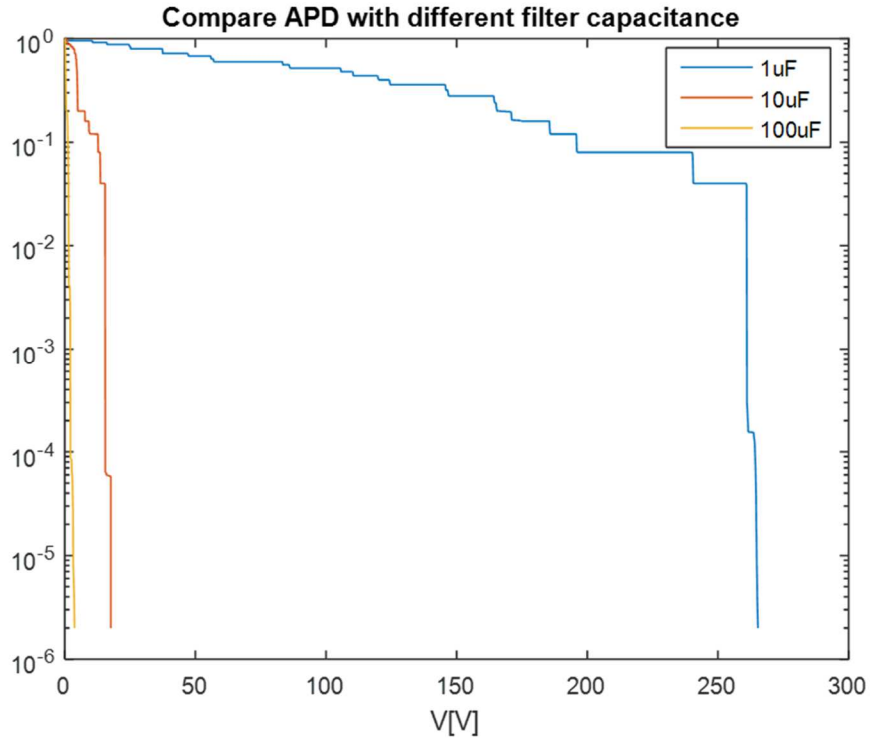


Figure 40-comparison the APD of the voltage measured at the LISN with different filter capacitance.

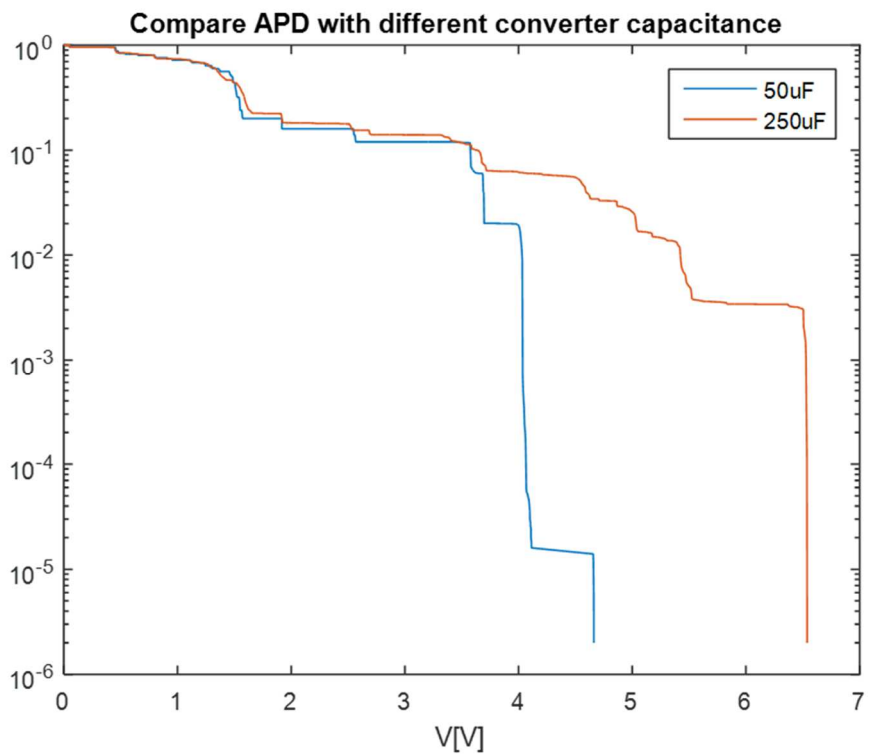


Figure 41-comparison the APD of the voltage measured at the LISN with different converter capacitance.

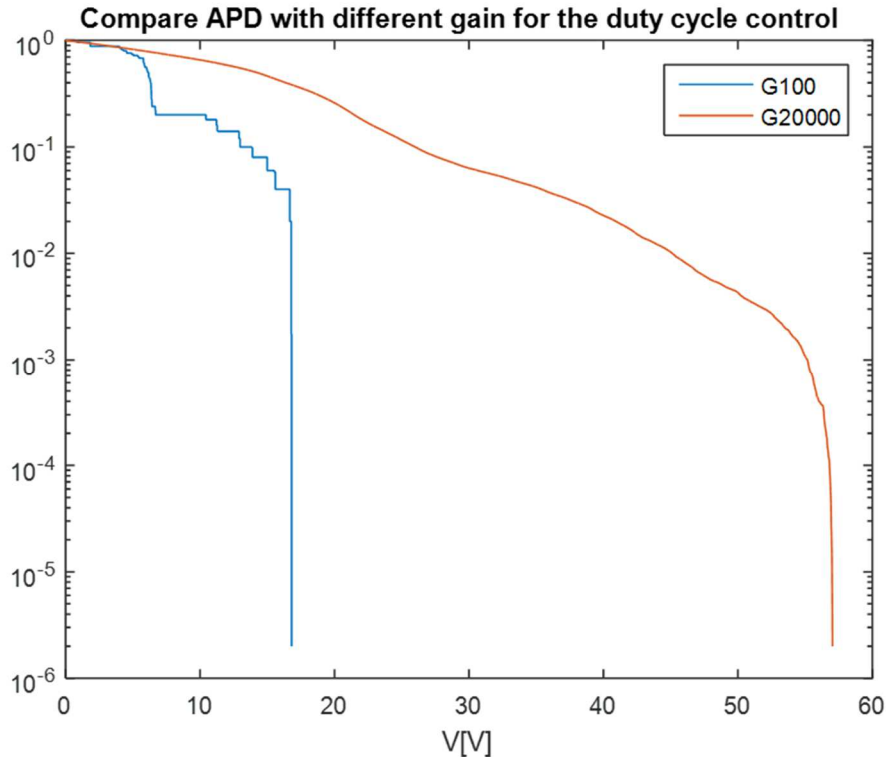


Figure 42-comparison the APD of the voltage measured at the LISN with different gain of the duty cycle control.

The APD results show variations at the different simulation configurations similar to the previous representations. It is possible to see that the voltages that the disturbances can reach are higher than the real measurement results. This is because in the simulation the peaks at the switching frequency and its multiples are very high.

However, it seems that there is an error in the calculation of the STFT using the FFT for every 200ms window. In fact, for example, the APD for $P=5230W$ and $V_{dc}=240V$, reaches 27V that means 148dB μV while in the STFT graph it reaches a value lower than 140dB μV . As already discussed for the figures 23, 25, 26 a way to improve the elaboration is to use directly the Matlab function “spectrogram”.

Other simulations and observations

As seen, the behaviour of the simulation circuit to the power variation is not the same of the real measurement. In fact, in the real measurement the disturbances are higher for lower requested power.

Trying to have the same behaviour between real measurements and simulation, the model's parameters can be changed and, in this case, the filter capacitance becomes 100 μ F instead 10 μ F and the filter resistance 1m Ω instead 10m Ω .

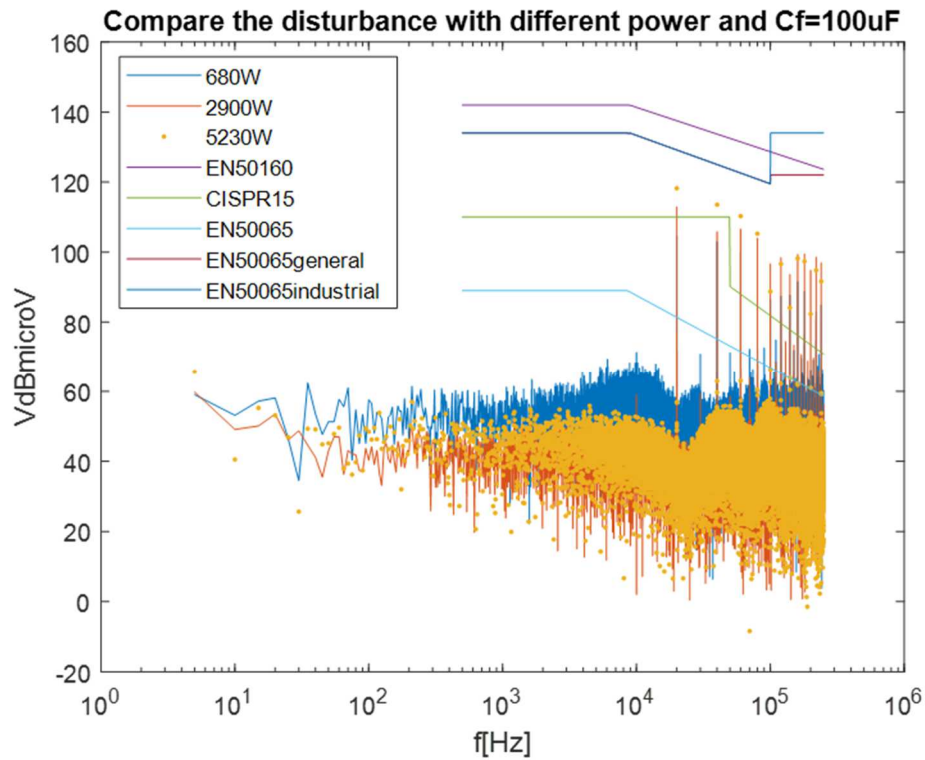


Figure 43

Table 4

<i>Data(240V)</i>	<i>LFSD_9kHz</i>	<i>LFSD_150kHz</i>	<i>x_E</i>
<i>P=680W</i>	<i>0.013</i>	<i>0.12</i>	<i>0.0016</i>
<i>P=2900W</i>	<i>0.003</i>	<i>0.46</i>	<i>0.0047</i>
<i>P=5230W</i>	<i>0.003</i>	<i>0.80</i>	<i>0.0081</i>

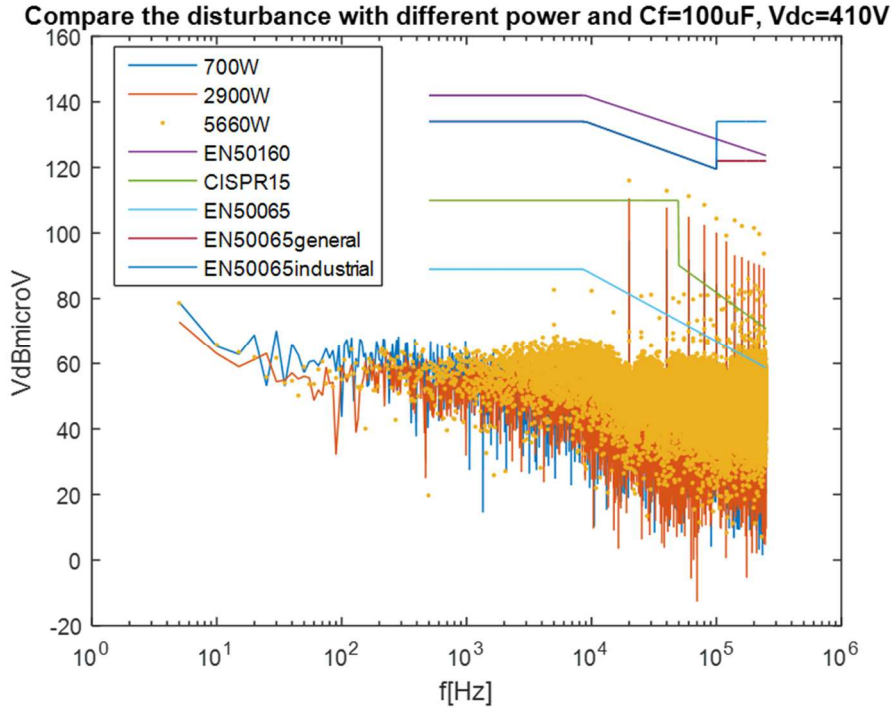


Figure 44

Table 5

<i>Data(410V)</i>	<i>LFSD_9kHz</i>	<i>LFSD_150kHz</i>	x_E
<i>P=700W</i>	<i>0.006</i>	<i>0.04</i>	<i>5.2*10⁻⁴</i>
<i>P=2900W</i>	<i>0.005</i>	<i>0.17</i>	<i>0.0017</i>
<i>P=5660W</i>	<i>0.010</i>	<i>0.34</i>	<i>0.0035</i>

It is possible to say that for the unknown real configuration of the converter it is tough to have the same behaviour between the real measurements and the simulations. For example, with a supply voltage of 240V (Figures 17 and 43) the behaviour is more similar than 410V (Figures 18 and 44). We can say this, looking the LFSD up to 9kHz, which, for the 240V simulations, shows an increasing of disturbances with a lower load. (The LFSD up to 150kHz maybe is not useful, for this consideration, due the very high peaks, in the simulations, at the switching frequency and its multiples, which are very influenced by the power requested).

Compare STFT and LFSD of Vin with different Windowing

Until now, rectangular windowing has been used. This windowing, which cut the signal at the ends of the window, could not put the signal equal to zero at

these points. This cutting without zero value can generate high frequency components that might fake the results.

To avoid this problem, the use of a different windowing that produce a zero value at the ends, as Hamming, Blackman, might be useful. In the next script a windowing presents in Matlab called “tukeywin” is used. The single 200ms windows of the signal are multiplied for the window with a same time extension (100000 data samples). Changing the second parameter, from 0 to 1, of the windowing, it is possible to change the shape of the window: with 0 is equivalent to a rectangular window, while 1 is equivalent to a Hann window.

```
VinF1=sqrt(2)/N*fft(Vin(t<=100000).*tukeywin(100000,0.01));
VinF2=sqrt(2)/N*fft(Vin(100000<t &
t<=200000).*tukeywin(100000,0.01));
VinF3=sqrt(2)/N*fft(Vin(200000<t &
t<=300000).*tukeywin(100000,0.01));
VinF4=sqrt(2)/N*fft(Vin(300000<t &
t<=400000).*tukeywin(100000,0.01));
VinF5=sqrt(2)/N*fft(Vin(400000<t &
t<=500000).*tukeywin(100000,0.01));
VinF6=sqrt(2)/N*fft(Vin(500000<t &
t<=600000).*tukeywin(100000,0.01));
VinF7=sqrt(2)/N*fft(Vin(600000<t &
t<=700000).*tukeywin(100000,0.01));
VinF8=sqrt(2)/N*fft(Vin(700000<t &
t<=800000).*tukeywin(100000,0.01));
VinF9=sqrt(2)/N*fft(Vin(800000<t &
t<=900000).*tukeywin(100000,0.01));
VinF10=sqrt(2)/N*fft(Vin(900000<t &
t<=1000000).*tukeywin(100000,0.01));
```

This windowing has been applied to the simulated voltage measured at the converter input.

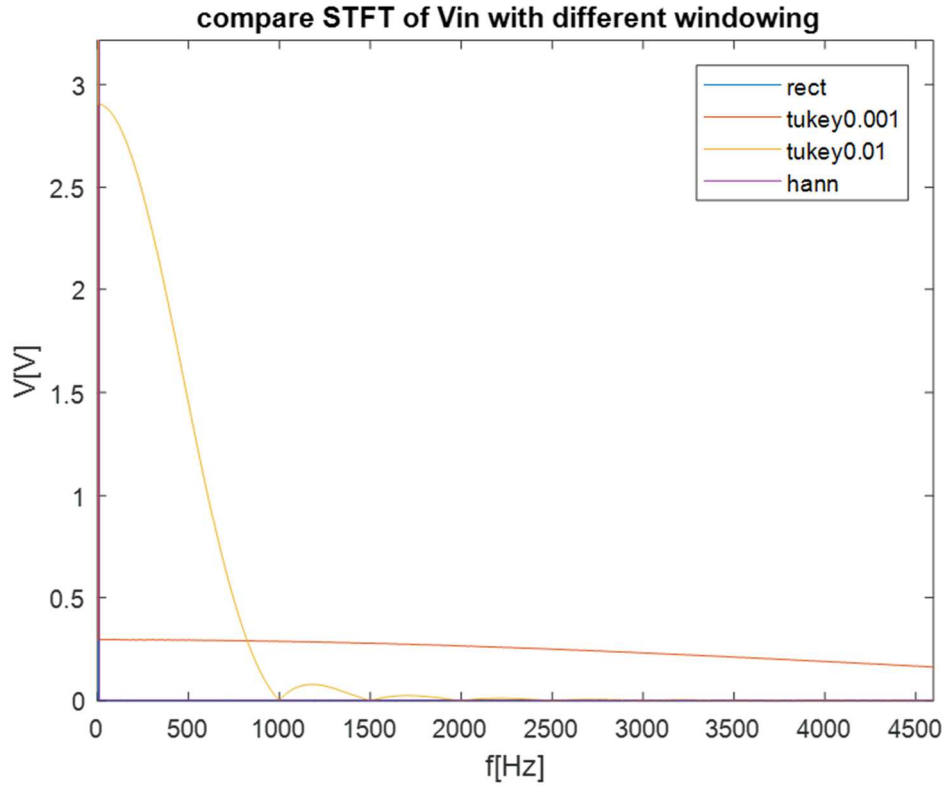


Figure 45

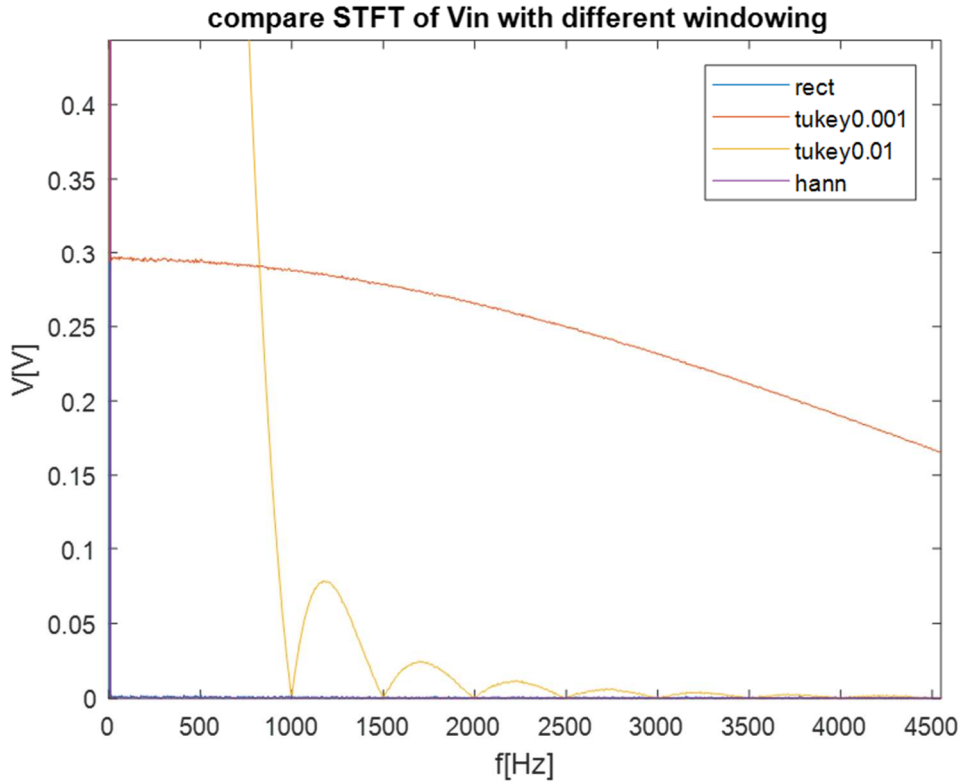


Figure 46

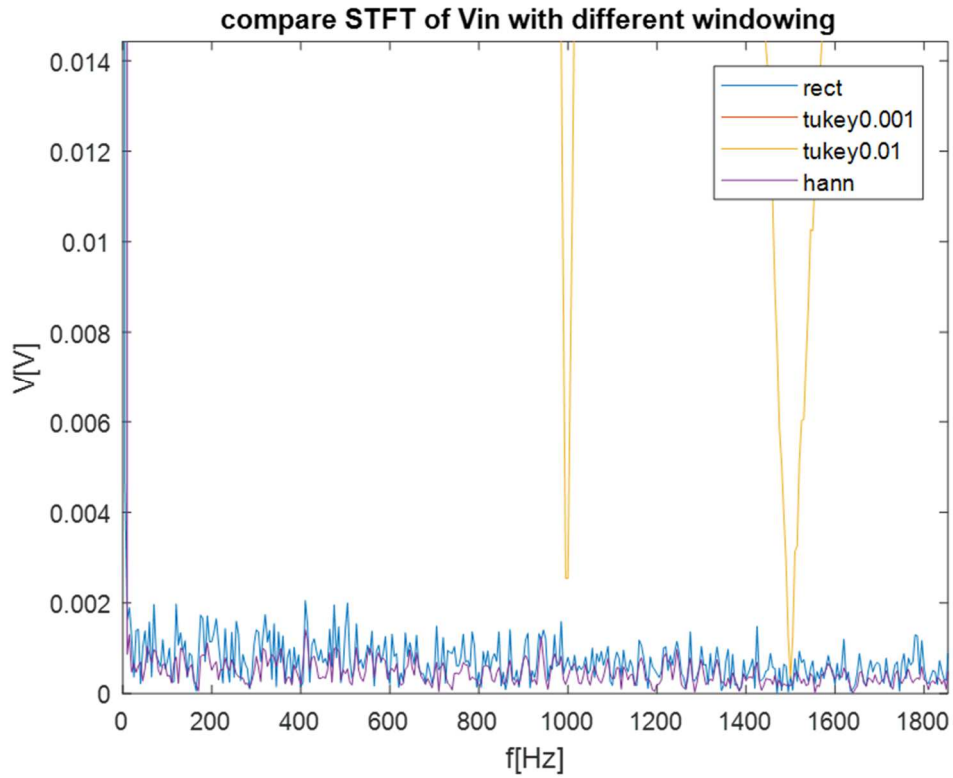


Figure 47

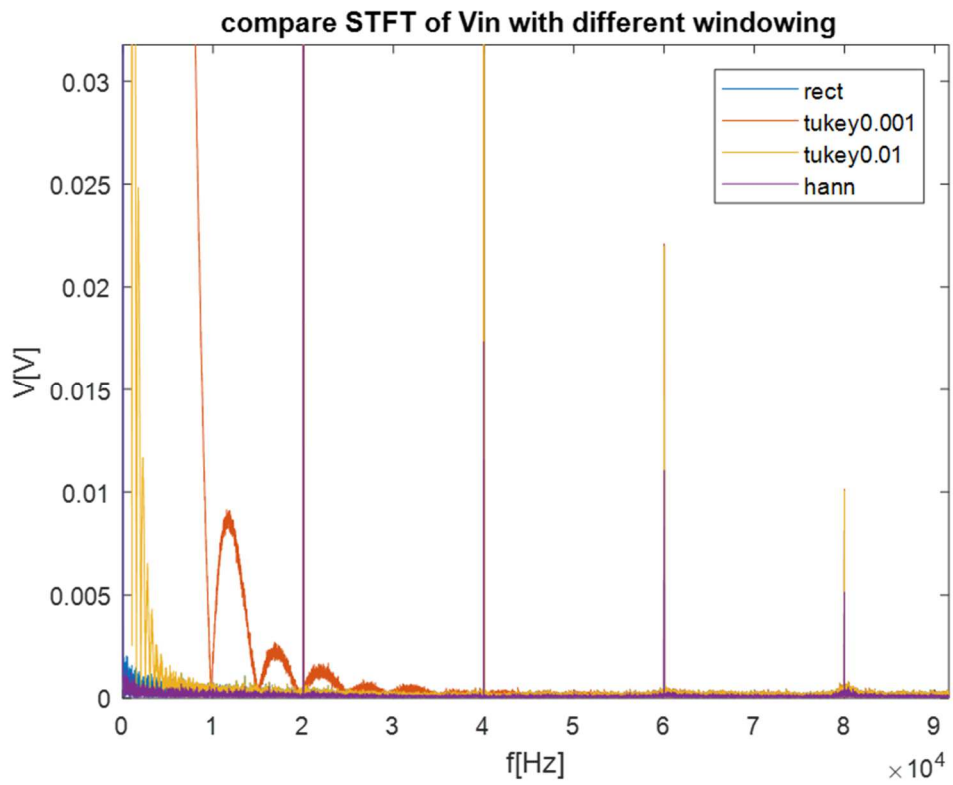


Figure 48

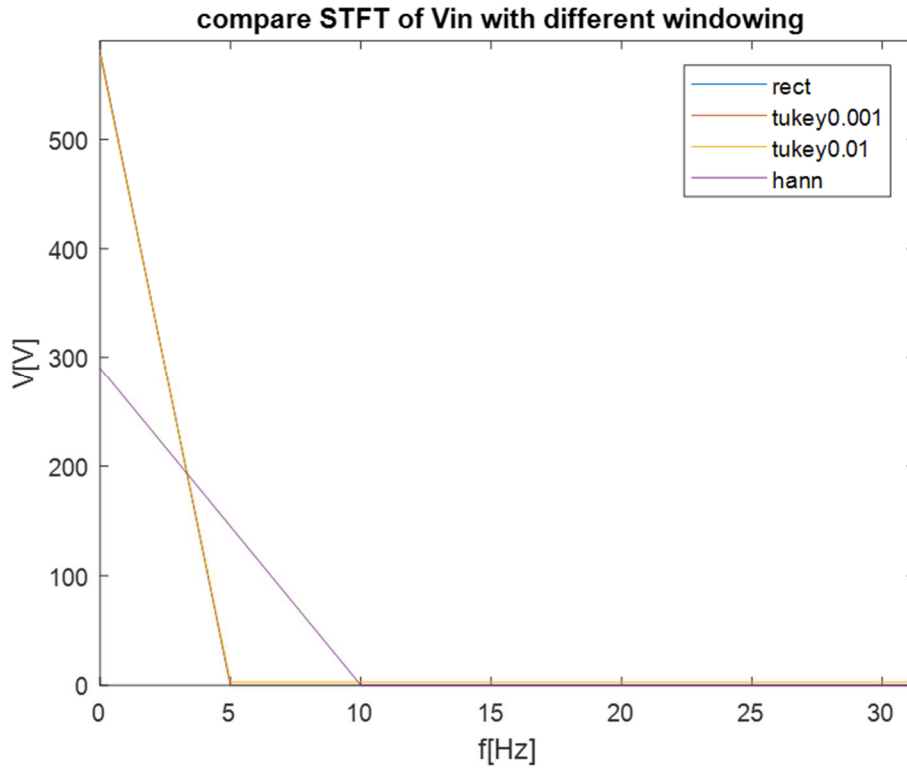


Figure 49

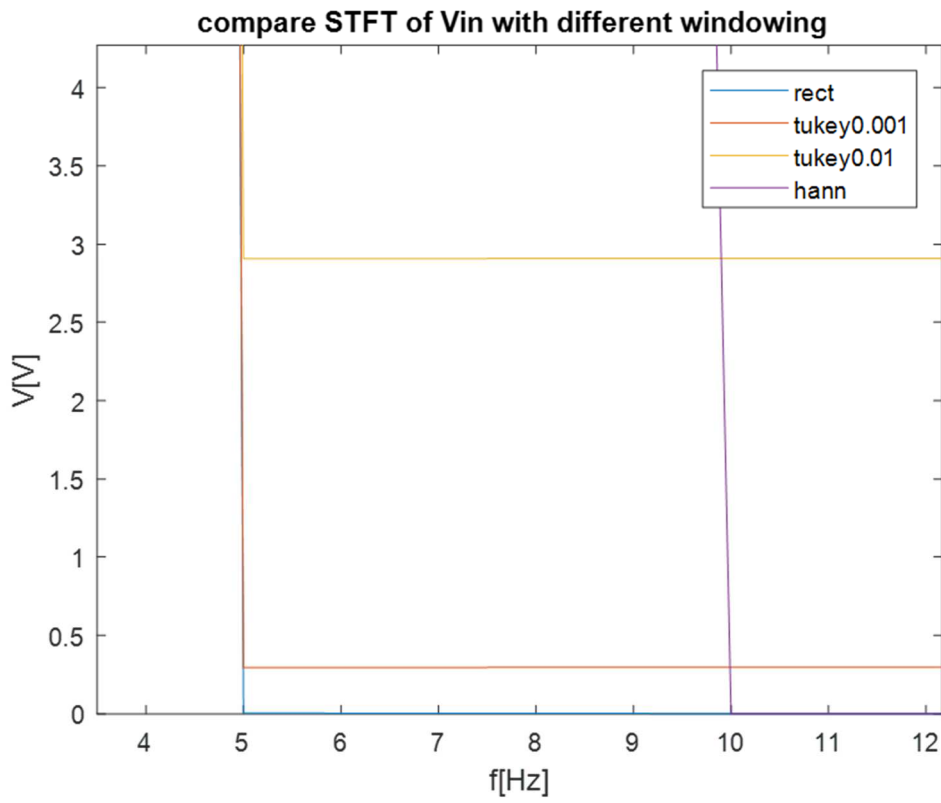


Figure 50

Table 6

<i>Data</i>	<i>LFSD 9kHz</i>	<i>LFSD 150kHz</i>
<i>Rectangular(tukey(0))</i>	<i>0.0057</i>	<i>0.0228</i>
<i>Tukey(0.001)</i>	<i>1.9609</i>	<i>1.9617</i>
<i>Tukey(0.01)</i>	<i>6.112</i>	<i>6.112</i>
<i>Hann(tukey(1))</i>	<i>35.36</i>	<i>35.36</i>

Figures 43, 44, 45, 46, 47, 48 show the STFT results of the input voltage of the converter of the simulation with a 700W load with $V_{dc}=410V$, calculated using different windowing. It is possible to see that the frequency domain behaviour of the windowing influences the global STFT and the LFSD (Table 6). The main differences that influence LFSD up to 9kHz are shown in figures 47 and 48. In fact, at 5Hz, the first point of calculation after 0Hz, STFT results are very different changing the parameter of the windowing: the narrower the window is in time domain (Hann), the higher are the STFT values at low frequencies. LFSD up to 150kHz are the same up to 9kHz because up to 9kHz it is already so high that other components do not influence the results anymore. To have right results maybe it might be worth not to take into account the frequencies until the frequency answer of the windowing influences the global STFT, maybe using windows with narrower bandwidth. However, using this method it might not be indicated for the calculation of LFSD because this parameter wants to calculate the distortion from low frequency.

To solve the problem above, in the LFSD calculation formula (54), it might be useful to subtract the value $Q[0]$, that is the one that gives problems, from every data in time domain of the quantity Q , and then doing the STFT of this new data input. This is done in the following script:

```
Xdc=1/(N1-500000)*sum(Vin(500000<t));%average DC component

Vinsub=Vin-Xdc;

VinF1=sqrt(2)/N*fft(Vinsub(t<=100000).*tukeywin(100000,0.01));
VinF2=sqrt(2)/N*fft(Vinsub(100000<t
&
t<=200000).*tukeywin(100000,0.01));
VinF3=sqrt(2)/N*fft(Vinsub(200000<t
&
t<=300000).*tukeywin(100000,0.01));
VinF4=sqrt(2)/N*fft(Vinsub(300000<t
&
t<=400000).*tukeywin(100000,0.01));
VinF5=sqrt(2)/N*fft(Vinsub(400000<t
&
t<=500000).*tukeywin(100000,0.01));
```

```

VinF6=sqrt(2)/N*fft(Vinsub(500000<t
t<=600000).*tukeywin(100000,0.01));
VinF7=sqrt(2)/N*fft(Vinsub(600000<t
t<=700000).*tukeywin(100000,0.01));
VinF8=sqrt(2)/N*fft(Vinsub(700000<t
t<=800000).*tukeywin(100000,0.01));
VinF9=sqrt(2)/N*fft(Vinsub(800000<t
t<=900000).*tukeywin(100000,0.01));
VinF10=sqrt(2)/N*fft(Vinsub(900000<t
t<=1000000).*tukeywin(100000,0.01));

```

Table 7

<i>Data</i>	<i>LFSD 9kHz</i>	<i>LFSD 150kHz</i>
<i>Rectangular(tukey(0))</i>	<i>0.0057</i>	<i>0.0228</i>
<i>Tukey(0.001)</i>	<i>0.0057</i>	<i>0.0228</i>
<i>Tukey(0.01)</i>	<i>0.0057</i>	<i>0.0228</i>
<i>Hann (tukey(1))</i>	<i>0.0034</i>	<i>0.0139</i>

The results of this calculation are shown in table 7: now LFSD results, using different windowing, are the same of the rectangular windowing, except for the Hann, which are lower, maybe due to the excessive cutting of the data; in fact, STFT shows that the harmonic peaks do not reach the same amplitude (Figures 46).

CONCLUSIONS

The increasing usage of the DC microgrid and other DC systems, as the HVDC transmission, led to the increasing of electronic converters as DC/DC and AC/DC. As a result of this, the electromagnetic disturbances are increasing, too. Every electronic device has to be electromagnetic compatible with the network and so, measuring and elaborating methods of these disturbances has to be developed and standardized. While in the frequency range up to 2kHz and from 150kHz there are standardizations, in the frequency range 2-150kHz there are not. In this thesis, methodologies for the measurement for this range are proposed.

It has been tried to adapt a LISN, used for measuring conducted emissions in the range 150kHz-30MHz, which might be an instrument to use also for the range 2-150kHz, but maybe changing the configuration of it because, as table 1 shows, the inductance and capacitance, at the lowest frequency border of 2kHz, have an impedance that might compromise the results.

For the disturbances elaboration, the tools of Matlab can be used to calculate the harmonic spectrum of the signals, using the algorithms of the Fourier Transform. The usage of the Fast Fourier Transform (FFT) and the Short Time Fourier Transform (STFT) have been studied, applying them to a steady state signal. Studying a steady state signal, there should not be differences between FFT and STFT and no differences between the calculation of the STFT using the Matlab function “Spectrogram”, or applying the FFT to each time-window, but, as shown in figure 23, 25 and 26, there are differences. Furthermore, as shown in figure 24, it seems that calculating the STFT applying the FFT to each time window, but using 100ms windows and not 200ms as many studies suggest, the results might even be worse (there is no the peak at 100kHz as in the other graphs).

Another topic studied in this work is the one of the different windowing that can be used. It has been seen that windowing might give STFT calculation errors due to their frequency behaviour. The variations of the harmonic amplitudes effect the calculation of the Power Quality parameters as the Low Frequency Sinusoidal Disturbance, as shown in table 6. To avoid these problems, a different calculation has to be used, obtaining the results shown in table 7.

Finally, it was tried to replicate the results of the real measurements with a simulation circuit made with Simulink-Matlab. Simulations can give a first approximation of the disturbances and their behaviour changing the circuit parameters, but, obviously, as was for this work, if the real configuration of the converter and its parameters are unknown, as the switching frequency, the simulation results will be different from the real measurement results.

The study of the conducted emission in the frequency range 2-150kHz is still a topic that needs further investigations and insights, comparing the results of different methods.

BIBLIOGRAPHY

- [1] M. Caserza Magro, A. Mariscotti, "Definition of Power Quality Indices for DC Low Voltage Distribution Networks", April 2006.
- [2] Irina Ciornei, Mihaela Albu, Mihai Sanduleac, Lenos Hadjidemetriou, Elias Kyriakides, "Analytical derivation of PQ indicators compatible with control strategies for DC microgrids".
- [3] Saron K. Meyer, Applied Research Group, "Power Quality Event Analysis using Wavelet Feature based Fuzzy Classification".
- [4] Marc Pous, Marco A. Azpurua, "Measurement and Evaluation Techniques to Estimate the Degradation Produced by the Radiated Transients Interference to the GSM System", December 2014.
- [5] Marc Pous, Ferran Silva, "APD radiated transient measurements produced by electric sparks employing time-domain captures", September 2014.
- [6] Marc Pous, Marco A. Azpúrua, Ferran Silva, "APD Oudoors Time-Domain Measurements for Impulsive Noise characterization", September 2017.
- [7] Frank Leferink, "Conducted Interference, Challenges and Interference Cases".
- [8] Marcello da S. Neves, Maynara A. Aredes, Hamidreza. Khezri, Elisa T. H. Ida, Maurício Aredes, "Advantages of Grid-Tied DC Microgrid"
- [9] E. O. A. Larsson, C. M. Lundmark and M. H. J. Bollen, "Measurement of current taken by fluorescent lights in the frequency range 2 - 150 kHz".
- [10] Giovanni Mazzanti, Massimo Marzinotto, "Extrud Cables for High Voltage Direct Current Transmission".
- [11] Wikipedia Images.